

Article

Composition, Distribution, and Attribution of Hydrochemistry in Drainage Systems in the North of Tianshan Mountains, China

Jia-Xin Zhang and Bing-Qi Zhu *

Key Laboratory of Water Cycle and Related Land Surface Processes, Institute of Geographic Sciences and Natural Resources Research, Chinese Academy of Sciences, Beijing 100101, China

* Correspondence: zhubingqi@igsnr.ac.cn; Tel.: +86-010-6488-9333

Abstract: The characteristics and sources of the hydrochemical composition of natural water are mainly influenced and limited at the basin scale by what factors, this has become a focal issue of environmental change in the middle latitude areas and even globally. In this study, three large drainage systems (Junggar, Yili, and Erlqis) in the north of the Tianshan Mountains were selected to study the hydrochemistry of different river basins and understand the relevant causes and attributions of different water bodies in arid environments in the Central Asian Orogenic Belt (CAOB). Natural water samples from the three drainage systems and their hydrochemical data, combined with literature data of the north and south Tianshan Mountains and surrounding areas, were systematically collected and comprehensively compared with other higher, middle, and low latitude watersheds with different climate conditions. The results show that the total dissolved solid concentrations in the CAOB drainage systems are generally higher than those of rivers in Chinese monsoon and humid regions, and also higher than the world average level. The relative concentrations of different ions are similar to those of rivers in the monsoon region of eastern China and most rivers in the world dominated by carbonate weathering. The ionic compositions of surface water bodies from different sub-basins in the study area are distributed near the Ca apex in the piper diagram, while those of phreatic and confined groundwater samples tend to the Na apex. The compositional differences in the anions are not like those in the cations, rarely distinguishable for these different water types. In a sub-drainage basin scale from I to VIII sub-basins in the study area, major ion concentrations and distributions in these basins are evidently heterogeneous. Almost all the cation and anion concentrations span > 1 order of magnitude, especially sodium and chlorine; however, the calcium and alkalinity concentrations and distributions are relatively homogeneous for some basins in the Junggar and Yili drainage systems. The relative homogeneity between anions and the relative heterogeneity between cations can be recognized in the ion chemistry of natural water samples between different types, indicating that the composition and distribution of cations in water is more conducive than those of anions to identifying the differences and commonalities between different regions. Atmospheric precipitation plays a key role on the hydrogeochemical process in the north of the Tianshan Mountains, and the elevation differentiation of chemical weathering and ion concentrations are closely related to it. The positive correlation between total solute flux and runoff cannot be explained by the dilution effect, indicating that hydroclimatic factors such as runoff and aridity have a strong effect in limiting the hydrochemistry of natural water bodies in the study area.



Citation: Zhang, J.-X.; Zhu, B.-Q. Composition, Distribution, and Attribution of Hydrochemistry in Drainage Systems in the North of Tianshan Mountains, China.

Atmosphere **2023**, *14*, 1116. <https://doi.org/10.3390/atmos14071116>

Academic Editor: Yael Dubowski

Received: 30 April 2023

Revised: 21 June 2023

Accepted: 26 June 2023

Published: 5 July 2023



Copyright: © 2023 by the authors. Licensee MDPI, Basel, Switzerland. This article is an open access article distributed under the terms and conditions of the Creative Commons Attribution (CC BY) license (<https://creativecommons.org/licenses/by/4.0/>).

Keywords: hydrochemistry; orogenic basins; chemical weathering; hydroclimatic factors; Tianshan Mountains

1. Introduction

The process of water–rock interaction, the so-called hydrochemical weathering of rocks, is one of the geological and surface processes with important environmental significance. It can not only change the surficial environment through the formation of a soil cover

layer [1,2], but also affect the surficial biogeochemistry cycle, such as the carbon cycle, by promoting the migration of soluble elements [3–8]. Some key environmental events have occurred since the late Cenozoic era, such as the uplift of the Himalaya–Tibetan Plateau, global cooling, and the rise of $^{87}\text{Sr}/^{86}\text{Sr}$ in seawater, all of which involve the changes of geochemical weathering related to the interaction between land surface water and rocks [9–15]. Studies have shown that the weathering of continental rocks dominated by hydrogeochemical process of river basins can promote the absorption and storage of atmospheric CO_2 through surface geosphere at different time scales, and currently the annual global CO_2 consumption due to chemical weathering may reach 0.252 Gt C [16].

However, there are still controversies in academic circles about the migration of different geochemical elements on the surface geosphere and their environmental effects. As an effective surficial process, what environmental factors are driving and limiting the hydrogeochemical process at the basin scale and how the process affects the atmosphere and climate at different spatiotemporal scales are still controversial scientific issues [13,17]. Due to the incongruence of water–rock interaction, especially the weathering of silicate rocks on a global scale [18], it has been widely recognized that different geographical units need to be integrated to solve the above scientific problems, in particular, the study of hydrochemistry on the scale of basins or drainage systems under diverse environments.

When the hypothesis of “tectonic uplift—chemical weathering intensification driving climate change” was proposed for global cooling in Cenozoic era [9,10], the hydrogeochemical processes and related environmental effects of orogenic regions with active tectonic movements in the world, especially the high-elevation regions in Asia, became the focus of academic attention. Up to now, hydrogeochemical research on basin or drainage system scales has been widely carried out in tropical/subtropical and karst areas [19–21]. Research data of large rivers and their main tributaries in the middle and low latitude monsoon areas, such as the Yellow River, the Yangtze River, and the Pearl River, are also rich [20,22–27]. Some studies have pointed out that the basin hydrochemistry and water–rock interaction in different environments in China are unique to each other due to the diversity of climatic and geological backgrounds [24,28]. However, at present, there are still few studies on watersheds or drainage systems from the Central Asian Orogenic Belt (CAOB), as well as the middle latitude westerlies in China, such as the arid basins from the Tianshan Mountains. Recently, it has been observed that although rivers in the middle and high latitudes of the Northern Hemisphere (NH) have a special mechanism of chemical weathering globally, such as the highest potential for carbonate weathering, their carbon fluxes through chemical weathering are the lowest [8]. This indicates that the hydrogeochemical processes in the middle latitudes of the NH are unique, but their characteristics and causes are still unclear. Therefore, it is of great environmental significance to carry out the hydrogeochemical research on typical basins in the middle latitudes.

The wide area in the north of the Tianshan Mountains located in the middle latitudes of China lies in the center of the Central Asian Orogenic Belt (CAOB) [29]. Tectonically, it is different from the circum-Pacific orogenic belt of sea–land collision and the Himalayan orogenic belt of land–land collision. It is a combination of fragments from ancient continents, island arcs, oceanic volcanic islands, passive continental margins, and other debris blocks [30,31]. Climatically, it is an important part of the global arid zone of mid-latitudes [32,33]. The three major drainage systems (Yili River System, Erlqis River System, and Junggar Basin System) in the north of Tianshan Mountains have great topographical gradient, complete climatic and vegetational spectrum, and significant ice/glacial and snow effect in high altitudes but less affected by human activities [34,35]. The hydrogeochemical processes and related environmental effects can have potential impacts on global climate change [32–34]. At present, hydrochemical studies on the drainage systems in the north of Tianshan Mountains have been gradually carried out [33–39], but most of them are case studies at the sub-basin scale, lacking systematic comparison and synthesis at regional and even global scales. There are still few analyses on the attribution of similarities and differences in the hydrochemistry over basin scale.

In this study, the hydrogeochemistry of natural water in the north of the Tianshan Mountains was analyzed, traced, and integrated, in order to comprehensively understand the characteristics, causes, and influencing factors of hydrochemical compositions of drainage systems in the northern Tianshan orogenic belt, and to explore the similarities and differences between drainage systems and other river systems in the middle latitudes of the NH and even on the global scale.

2. Background of the Study Area

2.1. Geographical and Climatic Environment

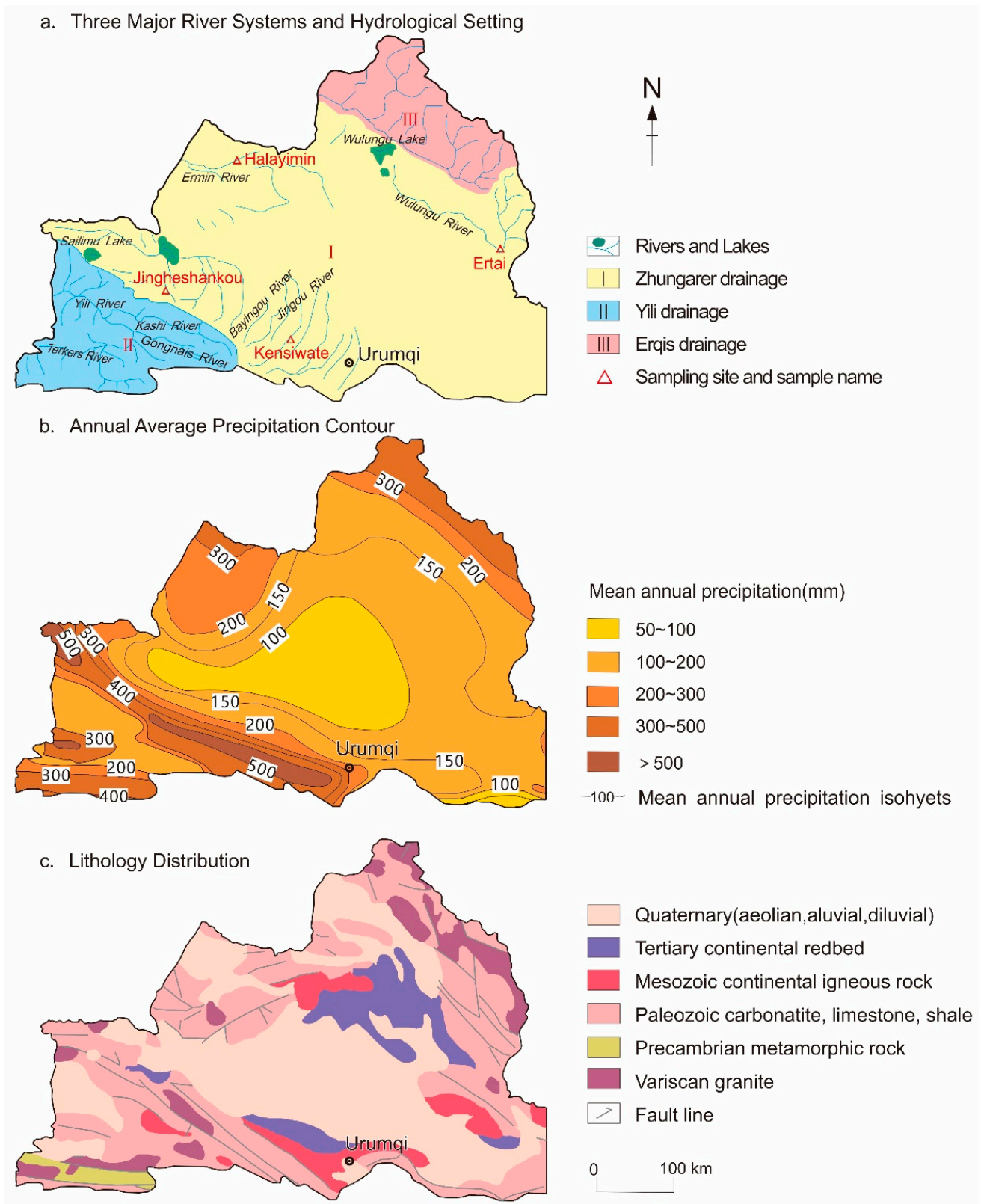
The area to the north of the Tianshan Mountains is located at the northwest border of China and is the geographical and drought center of the Asian continent. It is situated in the north of the Tianshan Mountains, the south of the Altai Mountains, and the east of a series of mountains and plains with an altitude of about 3000 m in northern Xinjiang. The longitudes and latitudes range between 78–90° E and 42–50° N, respectively, covering an area of about 603,000 km² (Figure 1). The topography of the study area is undulating and its elevation gradient is big, ranging from 500 m in the center of the Junggar Basin to more than 5000 m in the northern and southern margins. The central plain of the study area is relatively smooth, surrounded by rugged mountainous areas. The landscapes of the Gobi desert, grassland, sandy desert, and other Quaternary landforms are distributed in the central plain and cover a vast area, with densely populated oases dotted with human activities.

Generally, the area to the north of the Tianshan Mountains has a temperate continental climate. It is warm and dry in summer, cold and wet in winter, and has a distinct seasonality mainly controlled by the westerlies, as well as being affected by the Asian monsoon and Siberian air mass. The annual average temperature is about 5 °C, with the lowest temperature ranging from −10 °C to −20 °C in January, and the highest temperature ranging from 28 °C to 33 °C in August. The variation of seasonal temperature reaches 35 °C–45 °C, indicating a large interannual temperature gradient and difference [35]. Figure 1b shows the distribution of precipitation in the region, with an average annual precipitation of 100–500 mm/a, 60–150 mm/a in the central desert area and 200–500 mm/a in the surrounding mountainous areas. The atmospheric moisture is mainly brought by westerly winds from the west. The potential evapotranspiration rate is about 1000–3500 mm/a, varying with the seasons and the elevation gradient [35]. Compared with the area to the south of the Tianshan Mountains, the area to the north of the Tianshan Mountains has lower temperature, more precipitation, and little difference in evapotranspiration.

2.2. Hydrology and Geology

The area to the north of the Tianshan Mountains is mainly composed of three major drainage systems [40], namely the Junggar system in the central (I), the Yili system in the southwest (II), and the Erlqis system in the north (III) (Figure 1a). The Junggar and Yili drainage systems are inland water systems, and the rivers of the Erlqis drainage system eventually flow into the Arctic Ocean. Most of the rivers in the north of the Tianshan Mountains originate from the surrounding high mountain glaciers and snow cover, with most of the downstream areas located in deserts. Except for the rivers originating from the northern slope of the Tianshan Mountains, which mainly flow in a north–south direction, most of the rivers extend in an east–west direction. The hydrological/runoff distribution of rivers in the north of the Tianshan Mountains is characterized by a single-peak flow pattern with little interannual variation. The runoff in summer accounts for 50–70%, 10–20% in spring and autumn, and less than 10% in winter (Figure 2). Usually, thawing of snow/ice begins in early April and reaches the maximum flow flux around June. The peak water volume within a year is several tens of times that of the low water-flux period. The annual water distribution has a large variability (Figure 2), while the interannual variability is small (about 10%), indicating an overall stable hydrological status. The main distribution of water resources is about 17.09 billion m³ in the Yili region, 12.9 billion m³ in the Altai

region, and 6.16 billion m³ in the Tacheng region. The total surface water volume is about 43.57 billion m³ [22], and agricultural activities rely heavily on natural water resources.



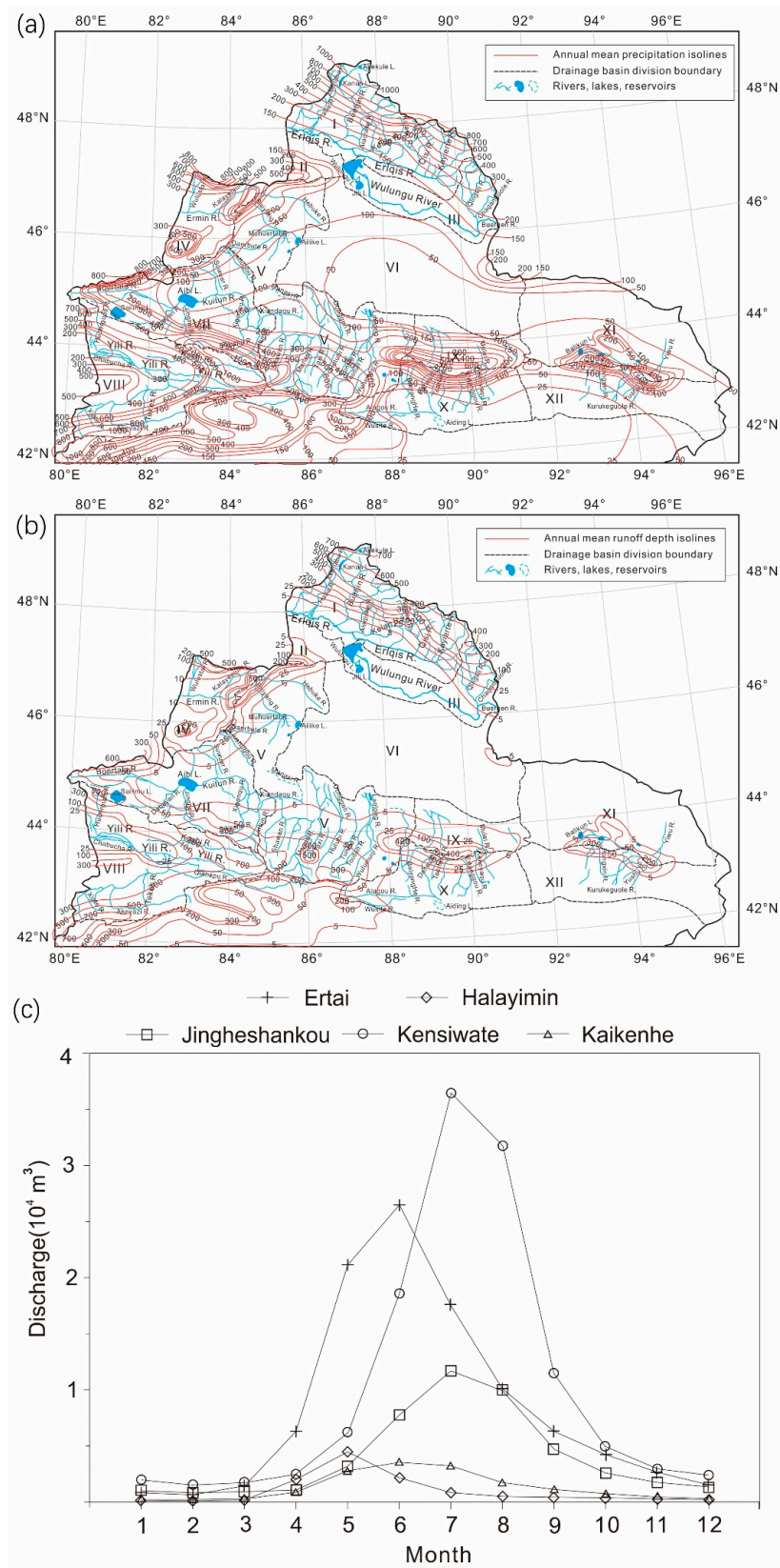


Figure 2. Isolines of the annual mean precipitation (a) and annual mean runoff depth (b) in the north of the Tianshan Mountains and the average seasonal distribution of multi-year runoff (discharge) of five rivers in the region recorded by hydrological stations (c). The geographical locations of the five hydrological stations in (c) are detailed in Figure 1a.

The area to the north of Tianshan Mountains lies in the area between the Siberian Plate and the Kazakhstan Plate, and is a part of the Central Asian Orogenic Belt (CAOB) and the Central Asian Metallogenic Belt (CAMP) [29,41], including terrestrial sedimentary crust, oceanic crust, marine volcanic island fragments, etc. The edge of the area is composed of exposed igneous rocks, metamorphic rocks, and loose clastic sediments, and the interior is covered by several kilometers of thick sediments forming stable blocks [30,31]. These blocks are composed of terrestrial sedimentary rocks (such as sandstone, shale, red beds, and coal), marine carbonate rocks, and evaporites [33] (Figure 1c). Silicate is the main rock type in the north of the Tianshan Mountains, and traces of evaporite also exist in the soil of the basin [36].

Among the three major drainage systems, the Junggar water system belongs to the Junggar Basin, which is an extension of the Paleozoic Kazakhstan plate and contains looser Quaternary and Tertiary aeolian sediments with a thickness of about 500–1000 m. There are many igneous rocks, Variscan granites, Carboniferous carbonates (C_1 , C_{2+3}), limestone, and Quaternary sediments in the Yili drainage system. The largest river in the basin is the Yili River, and most rivers in the water system eventually flow into the Yili River. The Yili River belongs to the inner flowing region of Central Asia and West Asia, originates from the Borokonu Mountains in the northeast and the Halik Mountains in the southeast, and flows into Kazakhstan through the Yili Basin [42]. Most rivers in the Erlqis drainage system converge into the Erlqis River, which is about 500 km long and is a large international river that stretches across China, Kazakhstan, and Russia, and ultimately flows into the Arctic Ocean. The Erlqis drainage system is mainly composed of Devonian marine carbonate rocks, clastic rocks (D_2 , D_{2+3}), Variscan igneous rocks, granites, and Quaternary sediments [33]. The annual runoff in the Yili and Erlqis drainage systems accounts for 27% of the total runoff in Xinjiang [33,42].

3. Research Methods and Data Sources

3.1. Research Methods

Although water–rock interactions are applied to the surface of rocks and minerals under microscopic conditions, hydrogeochemical processes in modern environments and over geological periods are usually studied at the watershed and stratigraphic/soil profile scales (geological profiling method) [18,43–46] due to the complexity of hydrogeochemical processes on the spatiotemporal scales [43]. At present, hydrogeochemical studies in modern environments are mainly focused on the abundance/flux variation (enrichment and loss) of easily migrated elements at the scale of the watershed unit [45], and then integrated and synthesized.

The research methods of hydrochemistry mostly use the chemical runoff method. The principle of this method is to measure the solute characteristics (such as TDS, TH, pH, ion concentration, etc.) of natural water at the river outlet or within the river channel, and analyze the regional hydrochemical status based on factors such as runoff, atmospheric input, rock outcrops, and human influence, so as to estimate the distribution of various types of water–rock interaction processes within the water system and the element migration fluxes generated. This method is universal and Meybeck [47] has verified it with a river applicable model. The results show that in a global scope, except for K^+ , which is greatly affected by human activities and other factors, the fluxes of other chemical elements or ions can fully reflect the hydrogeochemical process in the natural environment [16,45–50].

In this study, the chemical runoff method was used to study the water chemistry of drainage systems. The acquisition of field samples has been systematically carried out in the recent years. From August to September 2008, 2015, 2018, and 2022, natural water samples of different water types were collected from the north slope of Tianshan Mountains and the north area of Tianshan Mountains, including the upper, middle, and lower reaches of the main rivers, tributaries, lakes, reservoirs, springs, groundwater of mechanized wells, mountain snow, and rainfall in the plain areas. The collection locations, water sample types, sampling methods, water sample preservation and transportation,

analysis methods, and other information of parts of samples can be seen in Figure 3, the Supplementary Tables S1 and S2, and the references [33–38]. In the process of water sample analysis, the samples were firstly filtered at the sampling site, and the temperature (T), pH, conductivity (EC), electric potential (Eh), total dissolved solids (TDS), and other parameters of the water samples were measured with a portable water parameter instrument. The concentrations of major cations (Li^+ , Na^+ , NH_4^+ , K^+ , Mg^{2+} , and Ca^{2+}), major anions (F^- , Cl^- , NO_2^- , Br^- , NO_3^- , H_2PO_4^- , SO_4^{2-} , HCO_3^- , and CO_3^{2-}) and some trace elements in the water samples were analyzed in the laboratory. The relevant methods of instrument testing, sample preprocessing, and data correction can be found in detail in reference [34]. It should be noted that different types of natural water bodies were selected for comparative sampling to obtain the commonality and individuality of hydrochemistry in the basins under different environmental (climatic, hydrological, and geological) conditions. Although the main streams of large rivers in each water system are sampled in this study, it is more inclined towards the tributaries and mountain streams of these rivers, as tributaries can better reflect the characteristics of lithological, topographical, and geomorphological diversities of a large basin [51]. Based on the multiple-parameter data, this paper conducts a regional comparative analysis and summary by synthesizing data from other literatures.

A forward deduction model [14] was used in this study for the quantitative evaluation of hydrochemical contributions of different sources in the large three drainage systems in the north of the Tianshan Mountains.

3.2. Data Sources

In addition to the analysis data of natural water in the north slope of Tianshan Mountains and the area north of the Tianshan Mountains accumulated in our previous work, the data in this paper also include the latest literature data from other watersheds in the north of the Tianshan Mountains as the study area. The data sources are detailed in Tables 1 and 2. In this paper, the types of water samples, lithology, geology, topography, and landforms, as well as the scientific issues and research perspectives discussed, are comprehensively sorted and classified. The data of ionic and physicochemical parameters of different water samples ($n = 363$) involved in this study are detailly listed in the Supplementary Tables S1 and S2. The specific geographical locations and distributions of these water samples are shown in Figure 3. Based on these data, a comprehensive discussion, evaluation, and conclusion have been conducted in the following text.

Table 1. Summary of research issues on natural water chemistry in the northern catchment of the Tianshan Mountains.

Issues Involved	Classification	Reference
Types of water samples collected	River water (upstream, midstream, downstream, tributaries) Stream water Lake water Pond water Groundwater Artificial ditch water	[33–39,52–76]
Basin lithology	Carbonate rocks Silicate rocks Evaporites	[33–38,59–62]
landforms	Orogenic belt Sedimentary plain	[33–38,59,61–63]
Environmental/scientific issues and research perspectives	Ionic chemistry, Geochemistry Chemical weathering Water carbon, Carbon cycle Hydrology/Water Cycle, Water Quality, Water Environment pollution	[33,36,52,54,58,64,66–70,73,74] [33,34,36,55,59,76,77] [33] [33–35,37–39,56,57,63,65,71,72,75,77–80]

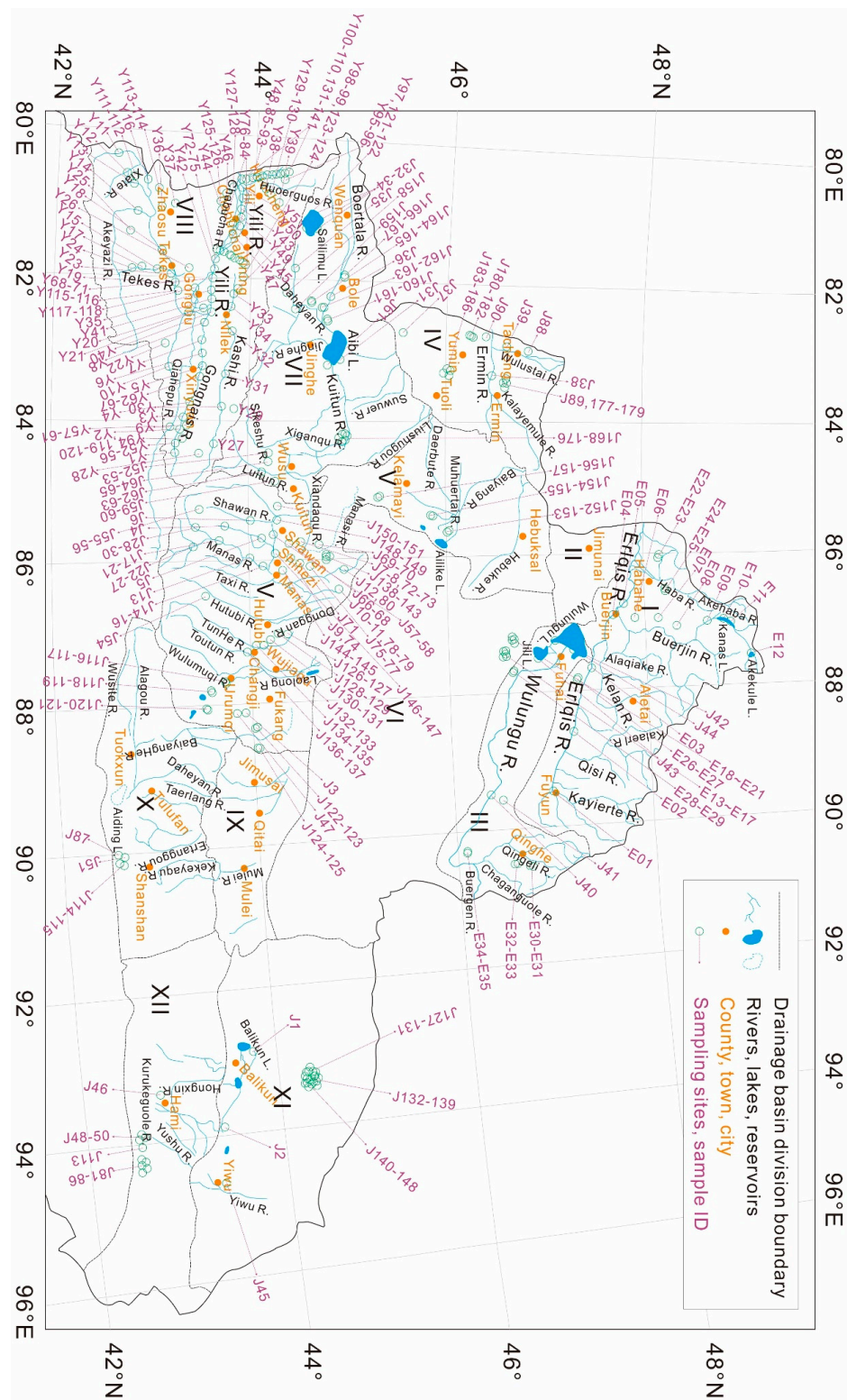


Figure 3. The spatial distributions of major drainage basins, rivers, and water sampling sites involved in this study in the north of the Tianshan Mountains. Note: I, Erlqis Basin (48,782 km² in area), II, Jimunai Basin (7656 km²), III, Wulungu Basin (25,355 km²), IV, Ermin Basin (20,806 km²), V, the middle part of the north slope of the Tianshan Mountains (81,433 km²), VI, Guerbantonggute Desert (85,143 km²), VII, Aibi Basin (49,812 km²), VIII, Yili Basin (56,953 km²), IX, the east part of the north slope of the Tianshan Mountains (17,707 km²), X, Tulufan Basin (36,398 km²), XI, Bayi Basin (56,522 km²), and XII, Hami Basin (40,677 km²).

Table 2. Summary of the literature for hydrochemical studies on large river basins in China and the world.

Regions	Water System/Catchment/River Basin	References
North of Tianshan Mountains	Yili River System, Erlqis River System, Junggar Water System	[33–36,38,81]
South of Tianshan Mountains	Keliya River Basin	[82–84]
	Yulongkashi River Basin	[82,83]
	Keziler River Basin	[82,85]
	Kashigarer River Basin	[82,86]
	Tarim River Basin	[82,87]
Hexi Corridor Area	Watersheds around the Tarim Basin	[83]
Yellow River basin	Heihe River Basin	[88]
	The middle and lower reaches of the Yellow River Basin	[89,90]
	Source Basins of the Qinghai–Tibet Plateau the Yellow River near Lanzhou hydrological station	[91] [91]
Yangtze River basin	Yangtze river basin	[23]
	the Yangtze River near the Nantong Hydrological Station	[92]
Monsoon zone (Anhui Region)	Jiuhuashan Granite Basin	[93]
West Siberian	Obi River Basin	[16,94]
North America	Loch Vale Basin	[95]
	Yukon River Basin	[96]
South America	Amazon River Basin	[97,98]
India	Yamuna River Basin	[99]
	Mohanadi River Basin	[100]
	Ganges River Basin	[99]
Poland	Northeast Poland Basin	[101]
Global	Global average or synthesis	[16,48,102,103]

In order to better understand the hydrogeochemical characteristics of the area north of Tianshan Mountains, based on the data of Tianshan Mountains, this paper also conducts a comprehensive comparison with the data of other middle latitude drainage systems around and other basins under different climate in the world. The basins involved are shown in Table 2, which also lists the sources of the referenced data and literature. Detailed data parameters can be found in the Supplementary Tables S1 and S2 of this paper.

4. Results

4.1. Composition and Distribution of Major Ions in Natural Water in the Study Area

Based on the analytical data in this study, the pH values of rivers in the north of the Tianshan Mountains range from 6.15 to 9.81 (Figure 4a), with a median value of 7.84 (Figure 4b), showing a neutral to slightly alkaline state (Figure 4a). The total dissolved solids (TDS) values range from 24.6 mg/L to 106,200 mg/L (Figure 4a), with an average value of 860 mg/L (Figure 4b). The average TDS values of the Junggar drainage system, Yili drainage system, and Erlqis drainage system are approximately 1160 mg/L, 212 mg/L, and 105 mg/L, respectively, ranging from freshwater (TDS < 1000 mg/L) to brackish water (1000 mg/L < TDS < 5000 mg/L), with a small portion of the natural water in the Junggar water system classified as hard saline water (Figure 4b). Compared to the spatial distribution of pH values, the TDS values show more significant spatial differences in the study area (Figure 4a).

The composition, distribution, and variation of major cation and anion concentrations of the studied water samples are shown in the fingerprint diagrams (Figures 5 and 6) and the Piper diagrams (Figure 7), respectively. The extreme values, median values, and mean values of major ion concentrations in different regions of northern of Tianshan Mountains are also shown in Figures 5 and 6. From the perspective of ion concentration values, the ion with the highest cation concentration is Ca^{2+} , followed by Na^+ , Mg^{2+} , and K^+ (Figures 5 and 6). The ion with the highest anion concentration is HCO_3^- , followed by SO_4^{2-} and Cl^- , and the concentration of NO_3^- ions is relatively low (Figures 5 and 6). There are evident spatial differences in the ionic compositions in different parts of the study area (Figure 5).

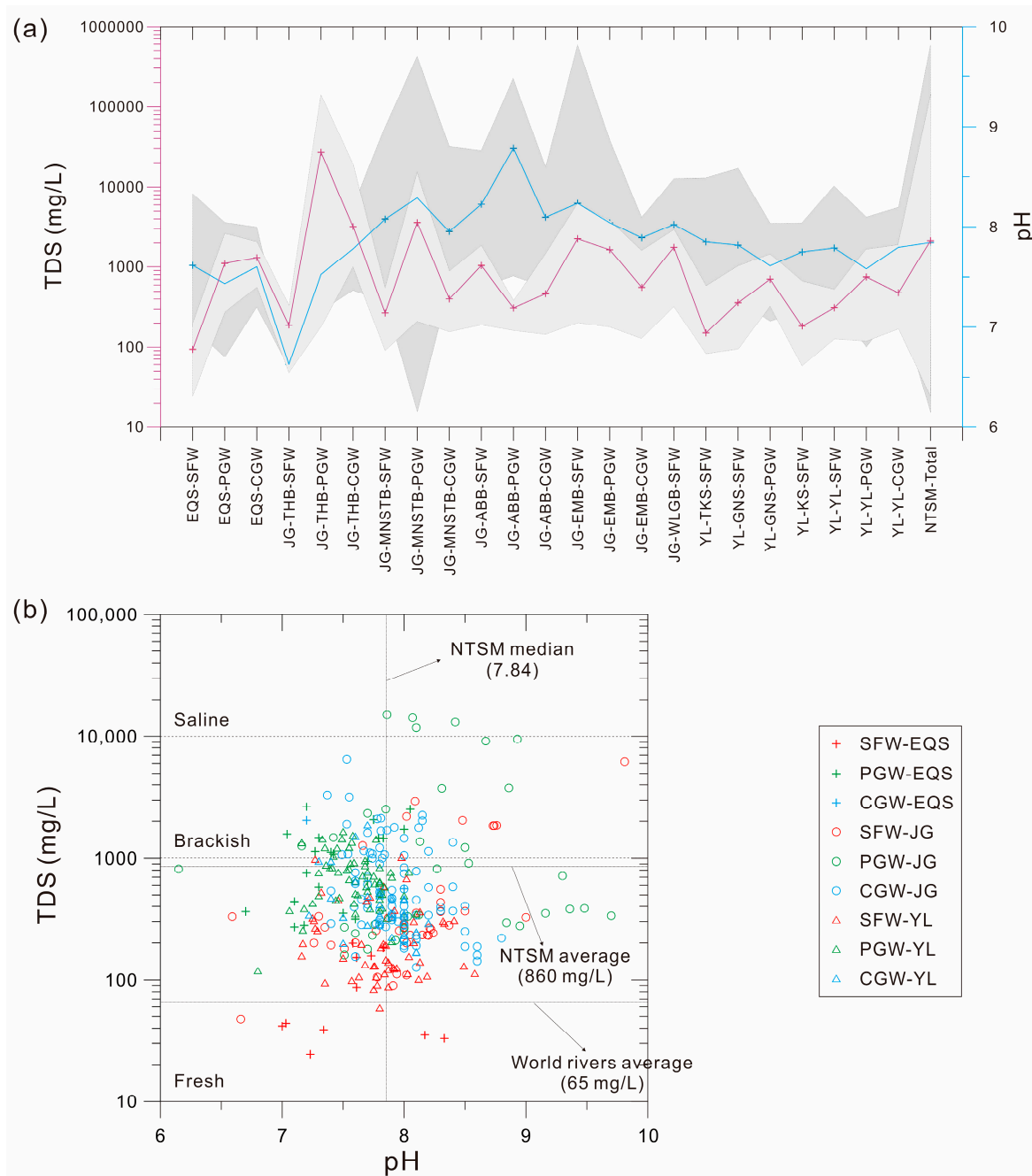


Figure 4. Ranges (max and min) and average values of TDS and pH of different water samples in the study area. (a) is the fingerprint diagram and (b) is the binary-variables diagram. The areas and sample types indicated by these capital letter abbreviations are detailed in the Supplementary Table S1.

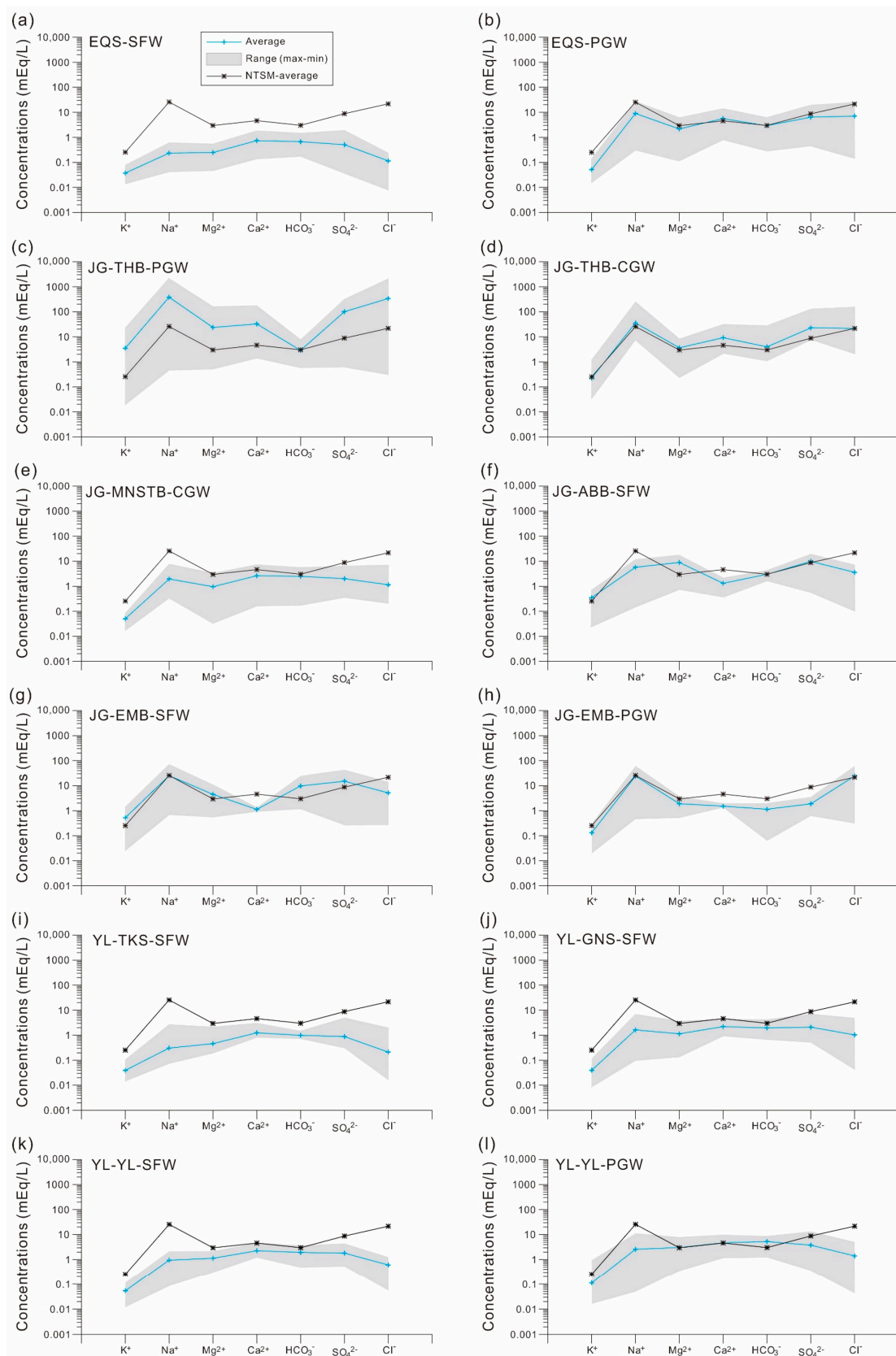


Figure 5. Cont.

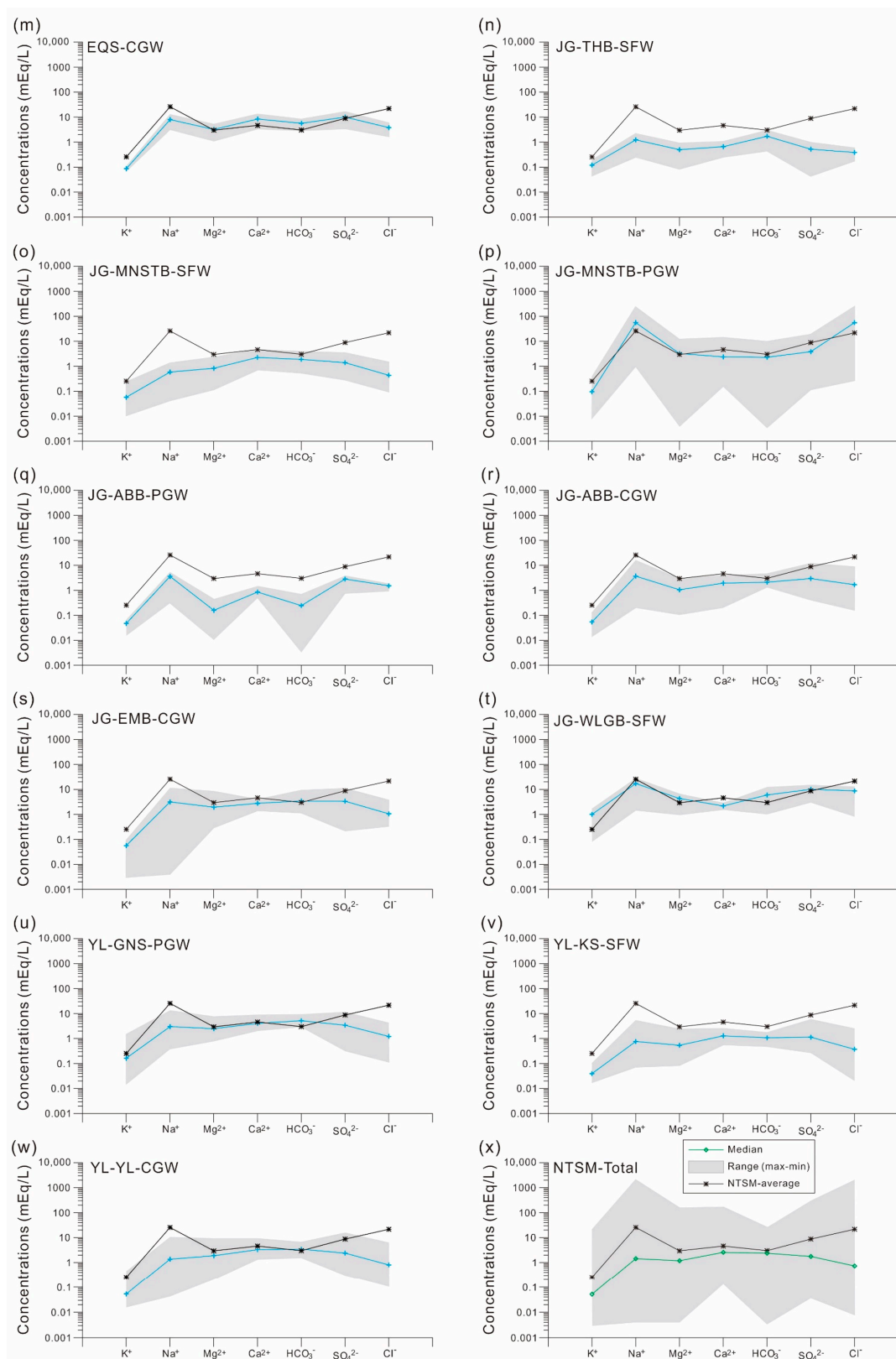


Figure 5. The fingerprint diagrams of the average and range of major ions of different water samples in different sub-regions of the study areas. The subfigures (a–x) correspond to different types of water samples from the sub-basins of the three major drainage systems, which are shown by capital letter abbreviations in the upper left corner of each subfigure. The areas and sample types indicated by these capital letter abbreviations are detailed in the Supplementary Table S1.

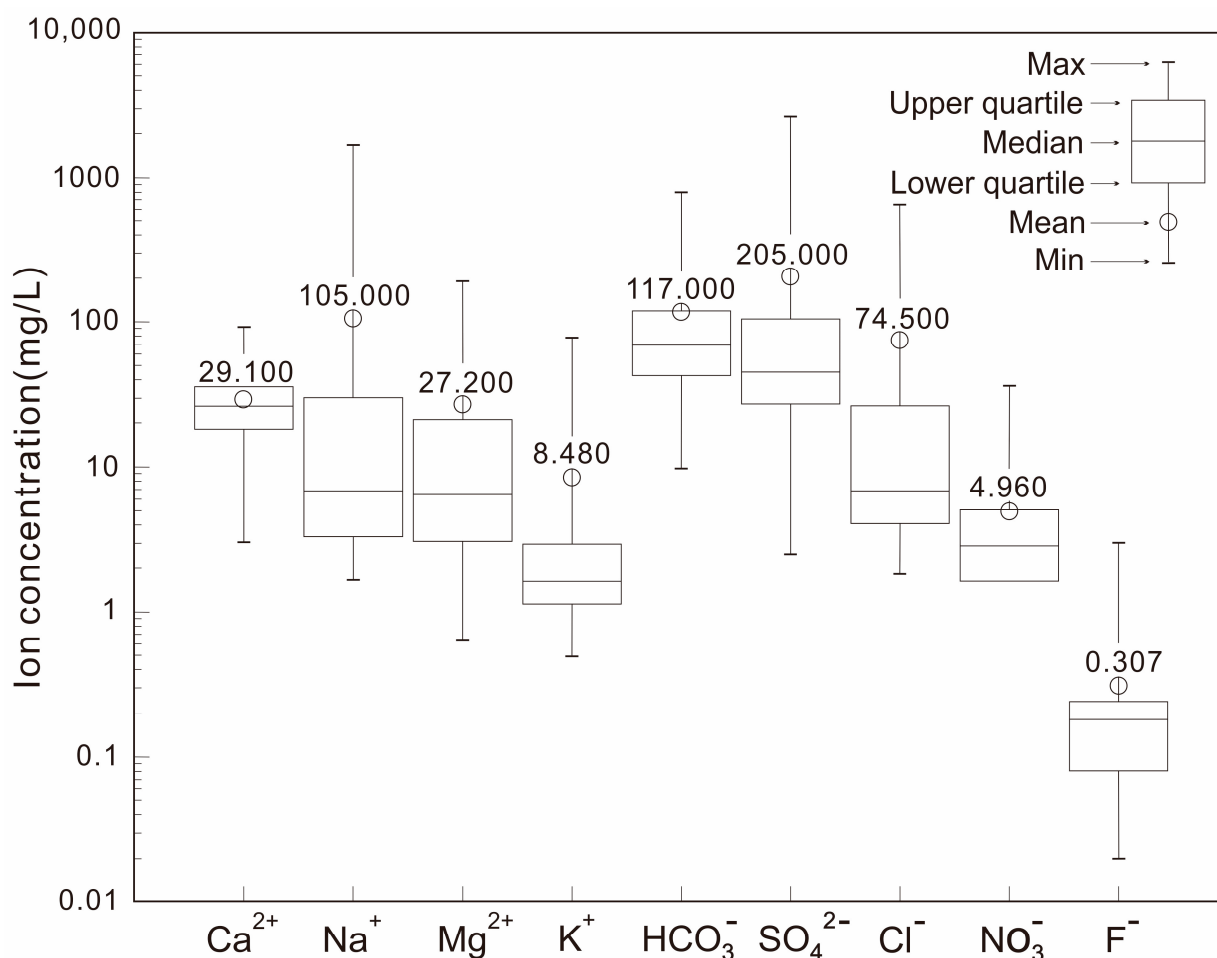


Figure 6. Distribution of main ion concentrations in natural water from the north of the Tianshan Mountains. To avoid excessive dispersion of variable distribution, ensure uniform display of data, and ensure the aesthetics of the graph, the ordinate of the figure uses a logarithmic coordinate system.

As shown in the Piper diagram (Figure 7) for the cations, the red data points (surface water samples) of the different river basins in the study area are distributed near the Ca apex (Figure 7a,c,e,g,i,j), while those of the phreatic and confined groundwater samples (green and blue data points, respectively) tend to the Na apex (Figure 7a,b,d,g,h). The magnesium concentrations do not clearly show such a difference among these waters (Figure 7). The compositional variations of the anions are not like the cations, rarely distinguishable for these different water types. However, the Yili water samples and the Erlqis surface water samples have lower chloride concentrations but higher alkalinities, compared to the Junggar water samples. In a sub-drainage basin scale (such as the I to VIII districts in this study as shown in Figures 3 and 7), major element concentrations and distributions in these basins are evidently heterogeneous (Figures 5–7). Almost all the cation and anion concentrations span > 1 order of magnitude. This is especially true for sodium and chlorine (Figures 5–7). However, the calcium concentrations and distributions are relatively homogeneous for some basins in the Junggar watersheds, such as JG-ABB-PGW, JG-EMB-SFW, JG-EMB-PGW, JG-EMB-CGW, and JG-WLGB-SFW (Figure 5q,g,h,s). Alkalinity concentrations and distributions are also relatively homogeneous in the Yili watersheds, such as YL-TKS-SFW, YI-GNS-PGW, YL-KS-SFW and YI-YL-CGW (Figure 5i,u,v,w).

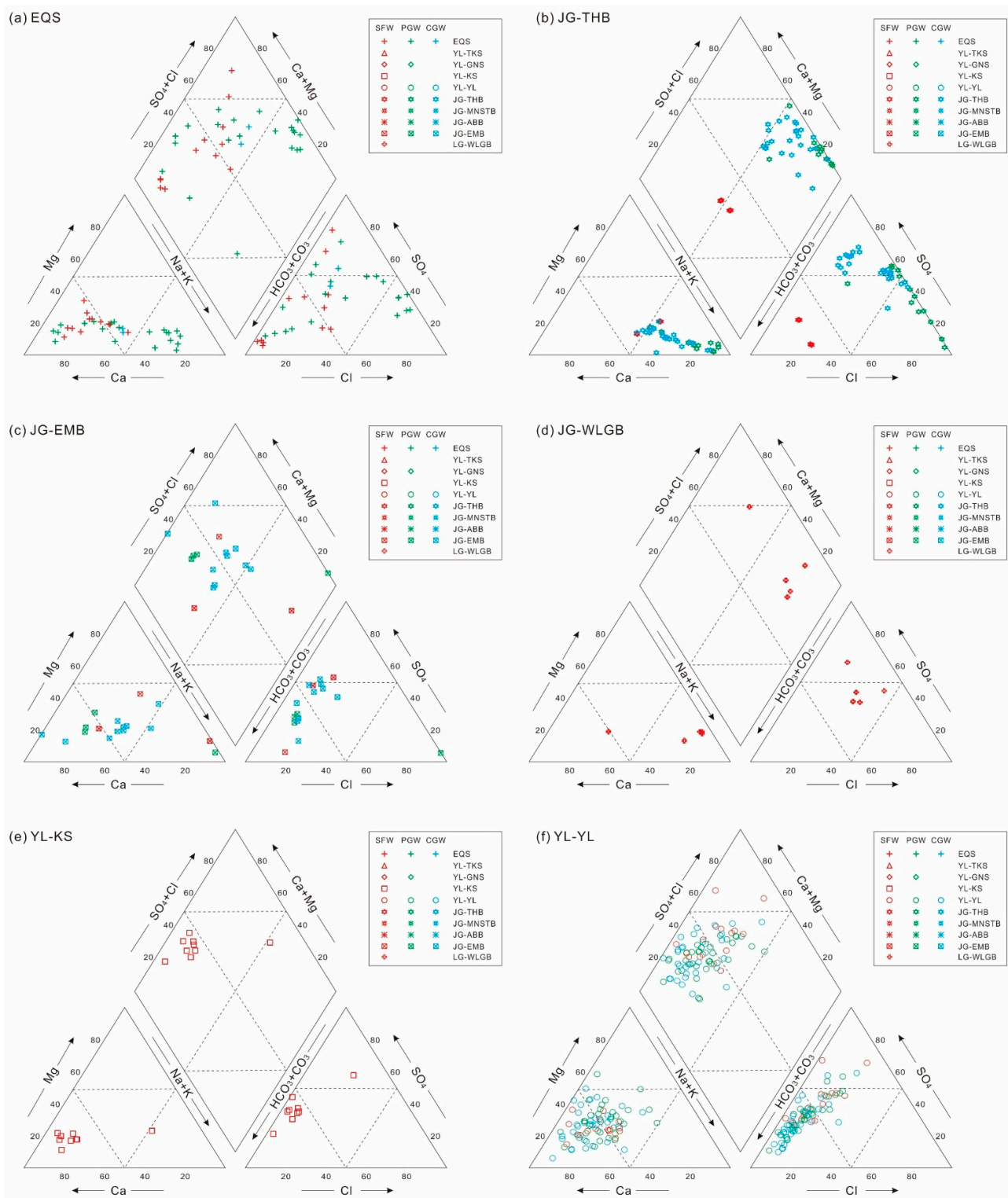


Figure 7. Cont.

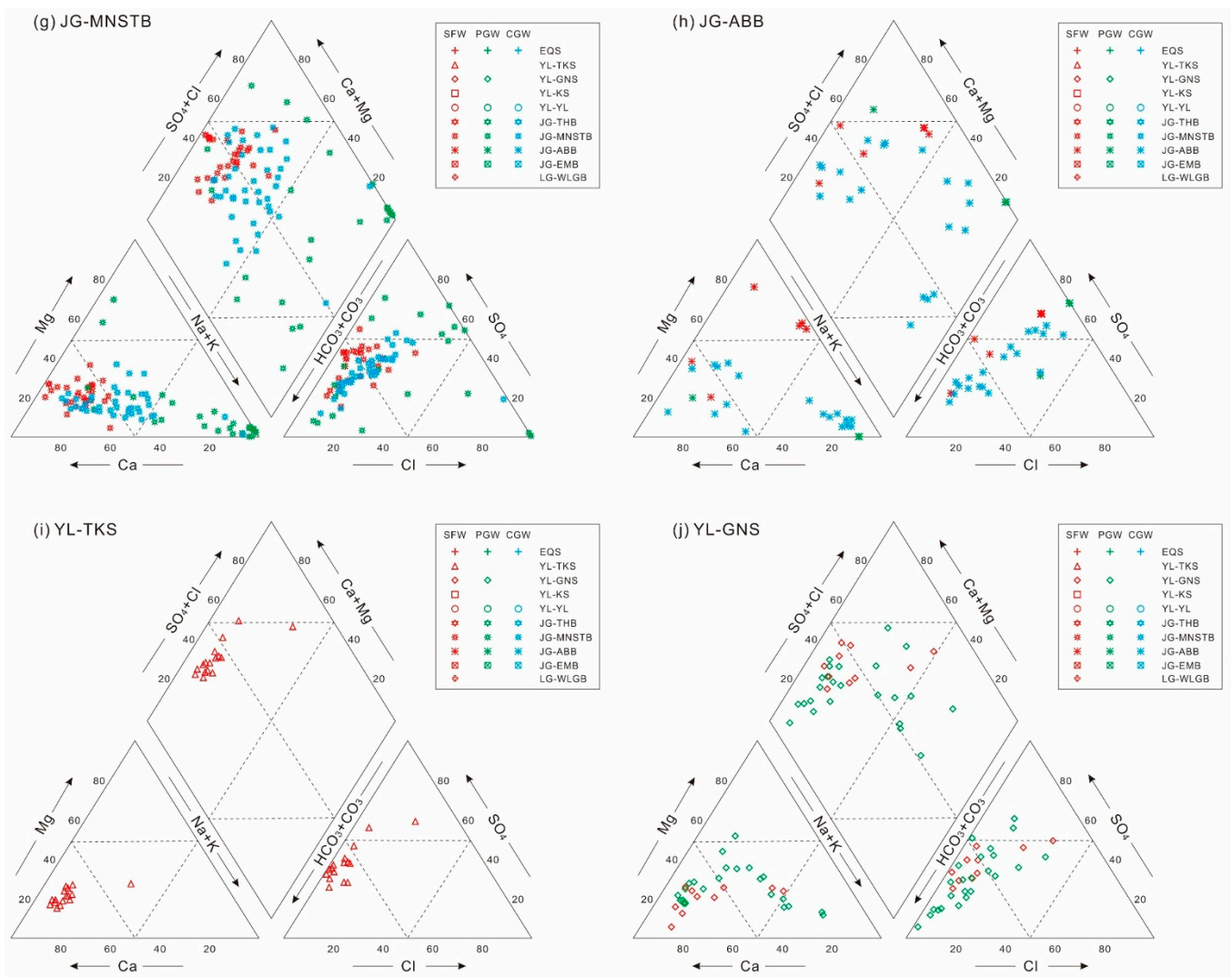


Figure 7. Piper plots of major ions of different water samples in different sub-regions of the study areas.

4.2. Regional Differences

As the geographical center of the Asian continent, the TDS values of the northern Tianshan Basins are not much different from those of water systems in the surrounding arid areas such as the southern Tianshan Mountains, the north Tibetan Plateau, and the central Alashan Plateau [82,104,105]. For example, the average TDS concentration of rivers such as the Keziler River in the southern Tianshan Mountains is about 737 mg/L ((270–1358 mg/L) [82,83,85]). The median TDS concentration of the Tarim River in the southern Tianshan Mountains is 531 mg/L [87]. According to Table 2 and the Supplementary Tables S1 and S2, the overall TDS concentration of various types of natural water (river water, lake water, groundwater, etc.) in the southern Tianshan Mountains water systems is 1589 mg/L [39,79,83], which is about two times that of water in the northern Tianshan Mountains. The TDS concentration of natural water in the central part of the Alashan Plateau [105], which is a middle latitude arid plateau along with the northern Tianshan Mountains, is comparable to that in the northern Tianshan Mountains. Therefore, the TDS concentration of natural water in the northern Tianshan Mountains does not exhibit strong heterogeneity in the arid region of Central Asia.

By comparing the TDS values of water systems in the study area, adjacent water systems, water systems at the same latitude, and other parts of the world, it can be seen from Figure 8 that the TDS values of rivers in the north of the Tianshan Mountains are generally higher than those in the monsoon region of eastern China, Sanjiangyuan region of

central China, and humid regions of southeastern China, and are 1.5 times higher than those in the upper reaches of the Yellow River (380 mg/L) [27,91,104], 2.8 times the Yangtze River (206 mg/L) [23], and even 8.9 times the world river average (99 mg/L) [48,49]. Among the 60 large rivers globally counted by Gaillardet et al. [16], only 6 rivers have TDS values higher than those in the north of Tianshan Mountains.

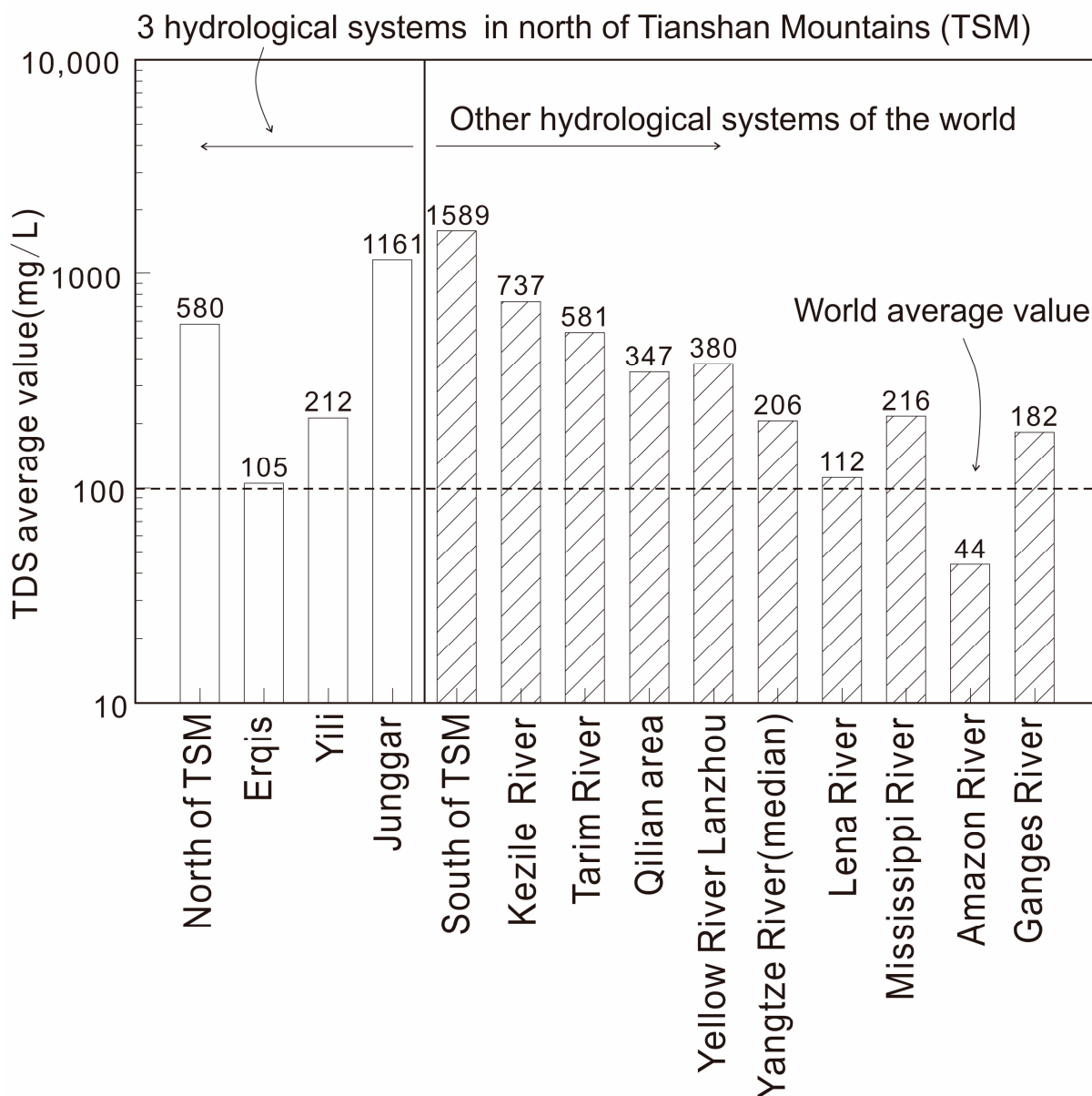


Figure 8. The average TDS values of the three drainage systems in the north of the Tianshan Mountains and the comparison with other drainage systems in the world. Note: the data used in this figure mainly comes from references [16,23,34,48,79,85,87,88,91]. In order to avoid the excessively scattered distribution of variables and ensure the uniform display of the data, a logarithmic coordinate system is used in the ordinate of this figure.

The relative homogeneity between anions and the relative heterogeneity between cations can be recognized in the above-mentioned ion chemistry of natural water samples between different types, indicating that the composition and distribution of cations in water is more conducive than those of anions to identifying the differences and commonalities between different regions. The total cations (TZ⁺) of different water systems are thus calculated. After integrating the data of this study with various data from the northern

Tianshan Mountains (Table 1 and the Supplementary Tables S1 and S2), it is found that a significant feature of the TZ^+ value of natural water in the north of the Tianshan Mountains is its large distribution range. Compared with the north of Tianshan Mountains and other arid areas such as the Tarim Basin in the south of Tianshan Mountains, the TZ^+ values are lower (2.3–6.6 meq/L) in the Gaizi River and Aksu River basins due to the high vegetation coverage, but are higher (3.6–24.6 meq/L) in the Keriya River and Yulong Kashi River basins due to the low vegetation coverage [83], and are higher (9.12–23.93 meq/L) in the Kizil River [85]. On average, the TZ^+ value of most rivers in the Tarim Basin is between 2.3–46.4 meq/L [83]. It can be seen that the TZ^+ values in arid basins of the northern and southern Tianshan Mountains are significantly higher than the world average (Figure 9), and the distribution range of the former is also relatively large.

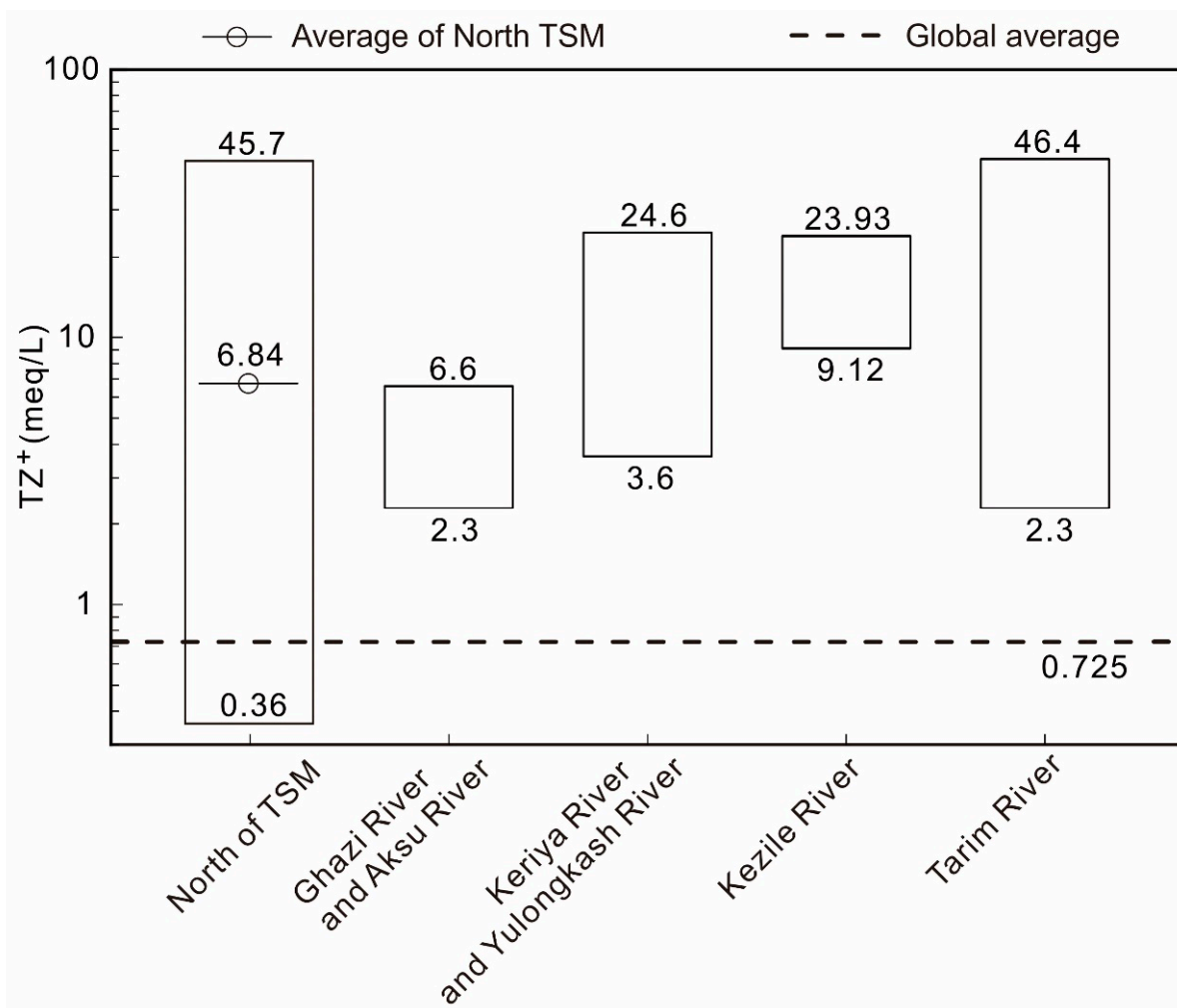


Figure 9. Distribution range of TZ^+ values in natural waters from the northern and southern regions of Tianshan Mountains. Note: in order to avoid excessively scattered distribution of variables and ensure the uniform display of the data, a logarithmic coordinate system is used in the ordinate of this figure.

Compared with other regions in the northern hemisphere (NH) (Figures 8 and 9), the concentrations of major ions in the rivers in the north of Tianshan Mountains are generally higher than those of tropical rivers at low latitudes, and are similar to the average levels of rivers in other middle-latitude temperate regions (about 20°–50° N) in the NH [22,34].

5. Discussion

5.1. Mechanism Controlling the Hydrochemical Compositions of Rivers in the Study Area: Rock Weathering, Climate, or Human Activity?

Under natural conditions, Gibbs [106] proposes that the hydrochemical composition of natural water is mainly controlled by three mechanisms: atmospheric precipitation input, rock weathering, and evaporative crystallization, which are mainly controlled by geological processes and climate effects. Other factors (such as terrain and vegetation) can only produce regional deviations under the influence of these three dominant factors [106]. On this basis, White and Blum [107] studied the hydrochemical characteristics of 68 large rivers worldwide and explored various factors that affect these characteristics. They pointed out that, on a global scale, the impact of rock chemical weathering on the watershed hydrochemistry is the most important. In addition, solutes in rivers may also come from atmospheric dry and wet deposition (dust and precipitation) and human activities [48,49,97].

Due to the distance between land and sea, arid areas are less affected by ocean water vapor. However, the existence of mountain glaciers/snow cover and arid climate due to tectonic and topographic factors makes the internal circulation of regional water vapor and the biogeochemistry cycle of erodible elements more intense. Therefore, it is more important to identify the hydrochemical causes on the water system scale in arid areas.

On the basis of the above analysis of the chemical characteristics of ionized water, the hydrochemical origin of the north of the Tianshan Mountains drainage systems is further discussed and analyzed. The following three aspects are mainly considered.

5.1.1. Input of Atmospheric Precipitation

In this study and the previous work, no trend of chloride concentrations decreasing with increasing distance from the ocean or decreasing with increasing precipitation has been found in the three drainage systems in the north of Tianshan Mountains, no matter for a single river basin or the whole drainage system [35]. This distribution pattern is similar to that of the Yangtze River Basin [23], indicating that the main source of chloride in water is not atmospheric precipitation, but more likely to be halite (rock salt) dissolution. Therefore, it is inferred that the input of atmospheric precipitation on the generation of solutes in the entire basin is limited.

5.1.2. Impact of Human Activities

The area north of the Tianshan Mountains is located in the inland region of Central Asia, and the population distribution is severely uneven, leading to its imbalance index being much higher than that of the monsoon region along the eastern coast of China [108]. Agricultural activities are concentrated in low terrain areas such as foothill plains and basins, forming typical oasis ecological landscapes; thus, the impact of human activities on local hydrology mainly focuses on the oasis and other low topographical areas [82]. It has been observed that nitrate concentrations in natural water bodies in the north of the Tianshan Mountains have no obvious correlation with total solute concentrations or runoff, but they have a strong correlation with intensive agricultural activities [35]. This feature indicates that although human activities may have a certain impact on water chemistry at the drainage scale, they are mainly reflected in local point-source or sheet-source pollution. Due to the limitation of its influence scope and the uncertainty of its influence intensity, this paper does not quantitatively estimate its contribution.

5.1.3. Influence of Rock Weathering

In the Gibbs' "flying-shuttle" model [106], which indicates the origin of water chemistry, the hydrochemical compositions of the area north of the Tianshan Mountains are mainly characterized by low $\text{Na}^+ / (\text{Na}^+ + \text{Ca}^{2+})$, low $\text{Cl}^- / (\text{Cl}^- + \text{HCO}_3^-)$ values, and moderate TDS values (Figure 10). This indicates that the hydrochemical composition of the area north of the Tianshan Mountains is dominated by chemical weathering of rocks (geological origin). Some areas are also affected by evaporative crystallization (arid climate

effect) or atmospheric precipitation input (humid climate effect) in different environments (climatic origin). The former is mainly reflected in the low terrain area (desert area) in the central part of the Junggar Basin, while the latter is mainly in the high elevation area with high precipitation, such as the mountainous and hilly areas of the three drainage systems [35].

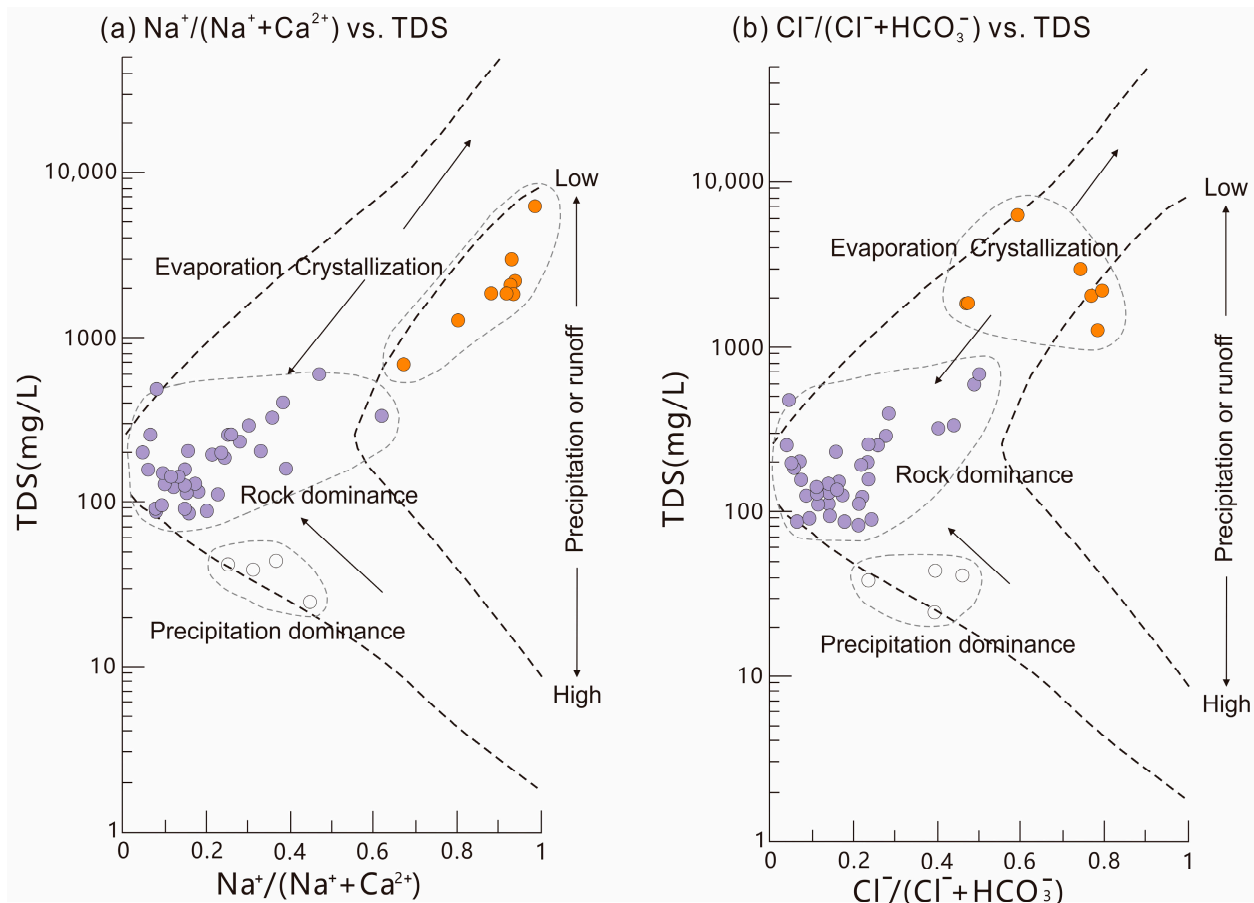


Figure 10. The Gibbs' "flying-shuttle" model cited from [106] for the formation of hydrochemical compositions of natural water in the north of the Tianshan Mountains.

Some researchers have found that when the Gibbs model is applied to identify the hydrochemical origin of various natural waters around the world, data points will fall outside the "shuttle" image [109–111]; that is, there are other factors (such as soil type, river channel shape, etc.) that affect the hydrochemical origin of natural water. Wu and Gibson [112] proposed a Ca-Na-TDS model to solve this problem, and further explained the contribution of other sources such as local precipitation and rock weathering input to Na+ concentration. The Ca-Na-TDS model built up in this study represents the "background" conditions of the atmosphere in northern China, as it uses the atmospheric precipitation data from the Waliguan meteorological basement station [113]. According to the analytical results in this study (Figure 11), rock weathering still plays a dominant role in the origin of hydrochemical composition of natural water in the north of the Tianshan Mountains, especially the weathering of calcium carbonate rocks and sodium silicate rocks. The effects of atmospheric precipitation input and evaporation are localized. The analytical results of the two hydrochemical models (Figures 10 and 11) are almost consistent.

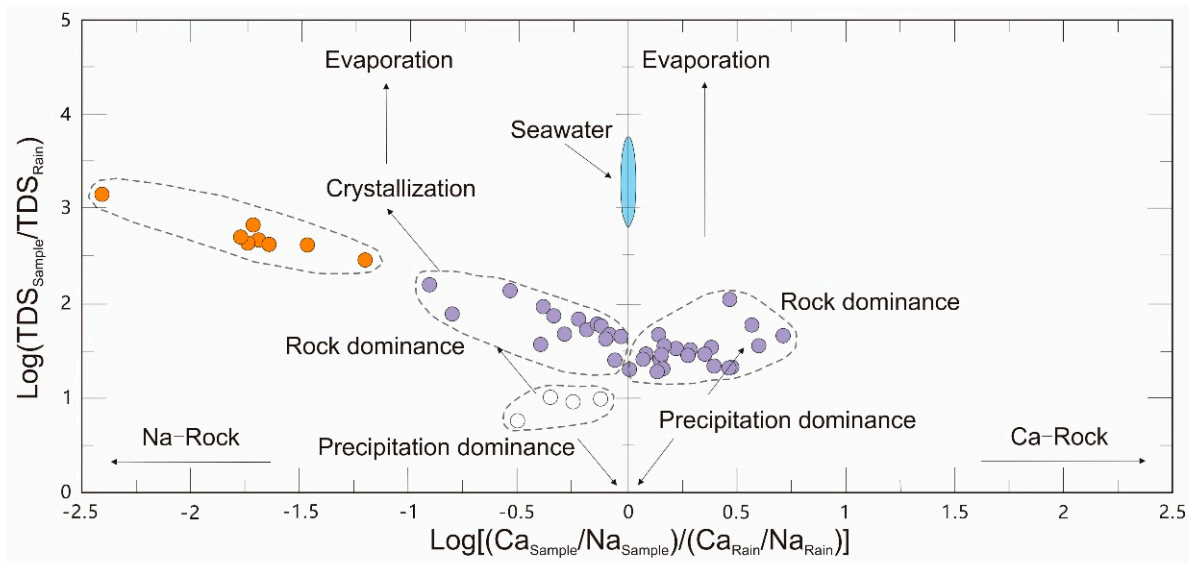


Figure 11. Distribution map of Ca-Na-TDS model cited from [112] for the formation of hydrochemical compositions of natural water in the north of the Tianshan Mountains.

5.2. Quantitative Contributions of Different Hydrochemical Sources

According to the analysis in the above, weathering of silicate rock, weathering of carbonate rock, evaporite dissolution, and input of atmospheric precipitation jointly contribute to the concentration of natural water solutes in the study area. In order to have a more intuitive understanding of the contribution ratio of the above sources, further quantitative division is made using the forward deduction method [14].

The water sample with the lowest Cl⁻ concentration in the tributaries of the Yili River is taken as the end-member sample imported completely by atmospheric precipitation to correct the Cl⁻ concentration in other natural water. After correction, assuming that X is the contribution rate of an ion from a specified source to the total cations in the basin, the contribution rate of precipitation in the solute in the basin can be calculated according to Formula (1):

$$X_{atm} = \frac{(X_{rain} \times Cl_{min}^-)}{Cl_{min}^-} \tag{1}$$

The subscripts atm, rain, and min in the equation represent the ion concentration of atmospheric input, atmospheric precipitation, and end-member ion, respectively.

Formulas (2)–(5) are used to calculate the contribution of silicate rock weathering:

$$TZ_{sil}^+ = 2Ca_{sil}^{2+} + 2Mg_{sil}^{2+} + Na_{sil}^+ \tag{2}$$

$$Ca_{sil}^{2+} = Na_{sil}^+ \times \left(\frac{Ca^{2+}}{Na^+} \right)_{sol} \tag{3}$$

$$Mg_{sil}^{2+} = Na_{sil}^+ \times \left(\frac{Mg^{2+}}{Na^+} \right)_{sol} \tag{4}$$

$$Na_{sil}^+ = Na_{nw}^+ - Na_{atm}^+ - Na_{eva}^+ = Na_{nw}^+ - Cl_{nw}^- - 0.10Cl_{atm}^- \tag{5}$$

In the formulas, TZ⁺ represents the total cation concentration; the subscripts sil, nw, and eva represent the contribution values of silicate rock, natural water, and evaporite, respectively; and the subscript sol represents the ratio of ion concentration in bedrock. Na⁺ in water is jointly provided by evaporite dissolution and silicate rock weathering. Ca²⁺ and Mg²⁺ contributed by silicate rock weathering are derived from Ca²⁺/Mg²⁺, Mg²⁺/Na⁺

ratios in soil and Na^+/Cl^- ratios in snow water and rainwater. The sampling data show that K^+ accounts for a very low proportion in natural water bodies in the study area, so the contribution of silicate rock weathering to K^+ is not included in the calculation.

The contribution of carbonate rock weathering can be calculated using Formulas (6)–(9):

$$TZ_{carb}^+ = 2Ca_{carb}^{2+} + 2Mg_{carb}^{2+} \quad (6)$$

$$Ca_{carb}^{2+} = Ca_{nw}^{2+} - Ca_{sil}^{2+} - Ca_{eva}^{2+} - Ca_{atm}^{2+} \quad (7)$$

$$Mg_{carb}^{2+} = Mg_{nw}^{2+} - Mg_{sil}^{2+} - Mg_{atm}^{2+} \quad (8)$$

$$Ca_{eva}^{2+} = SO_4^{2-}_{nw} - SO_4^{2-}_{atm} \quad (9)$$

The subscript carb in the equations represents the contribution value of carbonate rock weathering to the total concentration. The values of Ca_{sil}^{2+} and Mg_{sil}^{2+} are calculated from Formulas (4) and (5).

In the natural water, the remaining part is the amount of cations contributed by evaporite dissolution in addition to the above contributions.

According to the above calculation, the corresponding results are obtained. The cation contribution rate of atmospheric precipitation input is about 0.4–45.8% (average 8.9%), that of silicate rock weathering is about 8.9–26.7% (average 17.8%), that of carbonate rock weathering is about 14.9–44.6% (average 29.7%), and that of evaporite dissolution is about 9.8–74.3% (average 43.6%), which is consistent with the above qualitative analysis results.

In the three drainage systems in the north of the Tianshan Mountains, the order of contribution of different sources to natural water solute is: evaporite dissolution input > weathering input of carbonate rocks > weathering input of silicate rocks > atmospheric precipitation input. This proves the dominant role of evaporite dissolution and carbonate rock weathering. Similar contribution proportions have been found in adjacent basins and regions. For example, the order of contributions of different sources to natural water in the Keriya River basin in the south of the Tianshan Mountains is similar to that in the north of Tianshan drainage systems, with evaporite dissolution playing an absolutely dominant role, followed by carbonate rock weathering [84]. Evaporites also play a dominant role in the Keziler River basin, and gypsum is the most important source of evaporates [85]. The role of carbonate rock weathering in the middle and lower reaches of the river is enhanced, but it does not exceed that of evaporites [85]. In the world's rivers, about 50% of the dissolution load comes from the weathering input of carbonate rocks, 17.2% from evaporite dissolution, and 11.6% from silicate rock weathering [47]. The contribution proportions of silicate rock weathering (17.8% > 11.6%) and evaporite dissolution (43.6% > 17.2%) in the north of Tianshan Mountains are higher than the world average, but the contribution level of carbonate rock weathering (29.7% < 50%) is significantly lower, which may be the typical characteristics of drainage systems in the arid environment.

5.3. Environmental Factors Influencing the Hydrochemistry in the Study Area

In addition to geological and geographical factors such as tectonic activities, landforms, and lithologies [8,12,18,19], hydrogeochemical processes are also affected at the basin scale by diverse environmental factors such as climate, runoff, soil, and vegetation conditions [18,20,23,107,114–119]. The following attempts to analyze the environmental factors influencing the hydrochemistry in the area north of Tianshan Mountains.

5.3.1. Climatic Factors: Temperature, Precipitation, and Aridity

Firstly, some general phenomena are considered. The concentration of certain ions such as Cl^- and SO_4^{2-} in the study area is higher in low elevation areas, which may be the evidence that the dissolution of evaporite is prone to occur in desert areas. Furthermore, the weathering process of carbonate rocks is more intense at higher altitudes. The weathering

intensity of silicate rocks increases with the decrease of elevation [36]. These evidences indicate that the elevation-related factors can significantly differentiate the chemical weathering of different rocks in the study area.

The reason that hydrochemical processes differ at altitudes (or elevations) in the study area may be caused by temperature or precipitation. Although there is a general connection between temperature and altitude, the data analysis of existing studies shows that there is no obvious correlation between temperature and local ion flux in northern Xinjiang [36], so it is considered that temperature is not the dominant factor affecting the geochemical process of water in the region. However, studies have shown that there is a significant positive correlation between the average summer precipitation and the altitude (or elevation) in northern Xinjiang [35,36], with a large amount of precipitation concentrated in the mountainous area with higher elevation and linearly decreasing with the decrease of elevation [35]. In addition, it has been suggested above that the Cl^- in natural water in the study area comes from dissolution of rock salt rather than atmospheric precipitation input, and there is evidence that there is a positive correlation between the Cl^- concentration and the annual average precipitation in northern Xinjiang [35], which indicates that the climatic factor of precipitation affect the ion chemical composition of the water by affecting the chemical weathering process of rocks. Therefore, it is suggested that atmospheric precipitation plays a key role on the hydrogeochemical process in the north of the Tianshan Mountains, and the elevation differentiation of chemical weathering and ion concentrations are closely related to it.

The weak impact of temperature in the study area mentioned above is consistent with the conclusion of Gaillardet et al. [16] on the hydrochemistry of large rivers worldwide. This study has proposed that there is a certain correlation between temperature and chemical flux in many large river basins worldwide, but this correlation becomes weak in river basins with lower runoff depths (<100 mm/a) [16]. For most areas of the north of Tianshan Mountains (especially the Junggar and Erlqis drainage systems), the runoff depth is in this low value range (Figure 2), so the relationship between temperature and hydrochemistry is in a low correlation range in the study area.

However, in some river basins around the world, temperature may cooperate with precipitation to become a synergistical factor influencing hydrochemistry at the drainage system scale. There is a significant positive correlation between the logarithm of Na^+ concentration in the Yamuna River water and the reciprocal local temperature, indicating that the weathering of silicate rocks in the basin is strongly influenced by temperature [99]. However, the synergistical effect of the two climatic parameters on hydrochemistry has been demonstrated in more studies such that precipitation has a greater impact on hydrochemistry than temperature. According to Pinet and Souriu [120], the correlation coefficients between precipitation, temperature, and chemical weathering intensity are 0.63 and 0.25, respectively. With the increase of temperature, the influence of precipitation on the intensity of chemical weathering is intensified, and the effect of temperature on chemical weathering is also influenced by precipitation.

The synergistic effects of temperature and precipitation can control the hydrochemical process at the drainage system scale from another aspect. Drought is one of the representative effects of them. The arid climate attribute is composed of a combination of high evaporation (or high potential evaporation, a process closely related to temperature) and low precipitation. The areas north of the Tianshan Mountains are typical arid areas in the middle latitudes, where evaporation usually increases with the increase of drought degree (aridity), resulting in the decrease of water volume and the increase of ion concentration. When the ion concentration reaches saturation, crystallization leads to the precipitation of ionic minerals (salts). Carbonate, sulfate, and other components with low degree of saturation will precipitate first, then the evaporite minerals (salts) will precipitate and the corresponding ions will be removed from the water, thus changing the composition of water chemistry. The drought index (DI) is defined as a ratio between the average potential evaporation rate and the annual average precipitation in a region [36], which is calculated

and used to measure the degree of drought (aridity) in the study area (Figure 12). It can be clearly seen that there are positive correlations between DI and the logarithms of TDS, Na^+ , K^+ , SO_4^{2-} , and Cl^- concentrations (Figure 12). This indicates a close relationship between the degree of drought and solute concentration as well as hydrogeochemical processes in the study area.

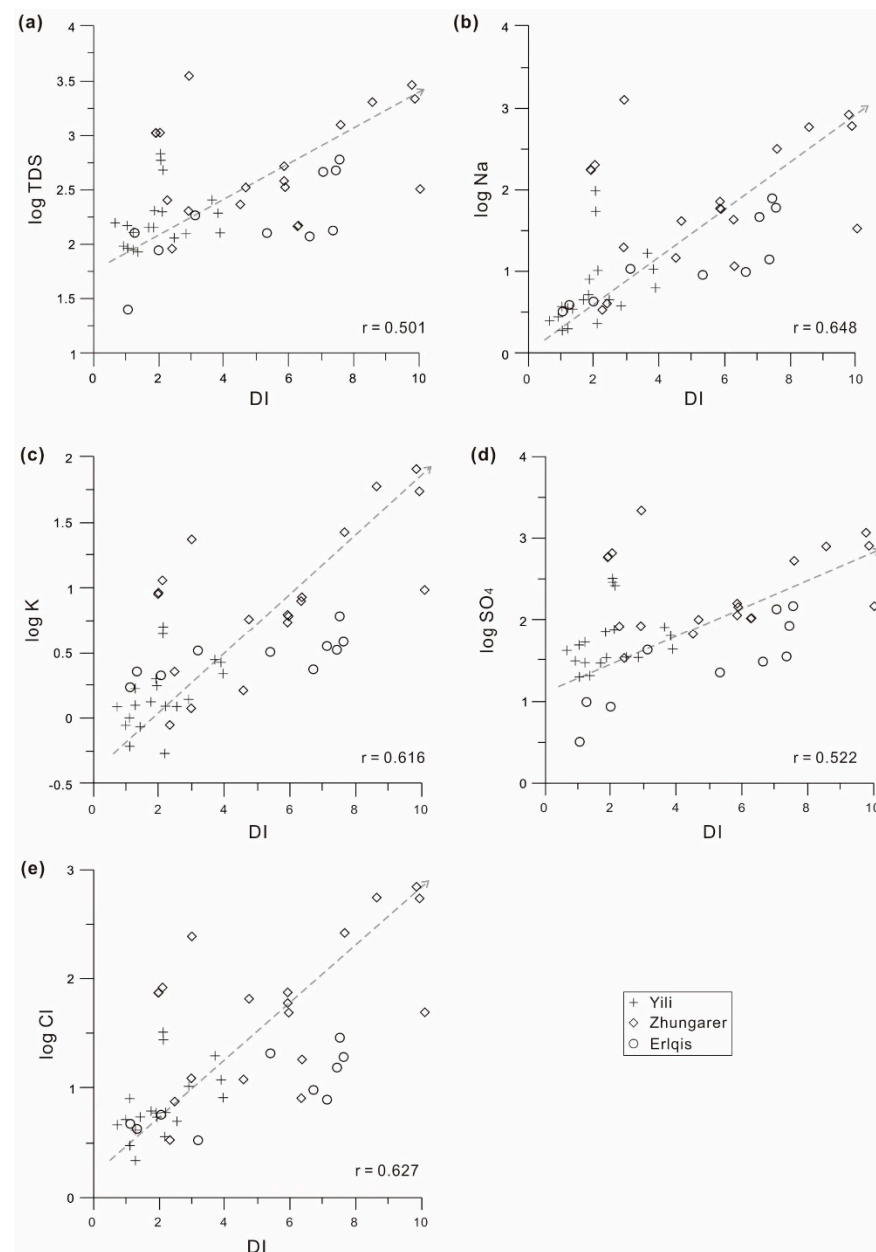


Figure 12. Relationship between major solute concentrations (in mg/L) and the drought index (DI) for the water samples from the area in the north of the Tianshan Mountains. Part of data are cited from [36]. (a) TDS vs. DI, (b) Na^+ vs. DI, (c) K^+ vs. DI, (d) SO_4^{2-} vs. DI, (e) Cl^- vs. DI. The vertical coordinates of these subfigures are logarithmic coordinates.

It is also important to note that the effects of temperature and precipitation are not always strong in all regions of the world. As Edmond and Huh [121] have argued, the influence of climatic factors is weak on the weathering of aluminosilicates in certain regions with stable tectonic activities. Riebe et al. [122] even argue that the rate of chemical weathering in areas with active tectonic activity and rapid physical erosion is almost completely controlled by tectonic activities, and the role of climate is very weak.

5.3.2. Hydrological Factors: Runoff

For arid areas with ice and snow meltwater as the main source of water supply, there are significant changes in the gradients of hydrological, hydrothermal, topographical, and geomorphological parameters between the upstream and downstream of rivers, and the hydrochemistry also changes accordingly. The concentrations of main ions in the upstream mountainous areas of the northern Tianshan river systems are obviously lower than those in the downstream basin. Na^+ tends to accumulate downstream, and the K^+/Na^+ values are higher in the upper reaches and decreased gradually in the lower reaches (especially in the Junggar drainage system). The $\text{Ca}^{2+}/\text{Na}^+$ values also show a decreasing trend from upland to lowland [35].

This phenomenon may have certain relationship with the changes in elevation or the different intensity of evaporation between upstream and downstream, but it may be mainly influenced by runoff factors. To demonstrate the possibilities, the relationship between hydrochemical solute fluxes and runoff data of different river systems in the north of Tianshan Mountains is analyzed and shown in Figure 13. It can be seen that there is a significant positive correlation between the TDS flux and runoff data in Figure 13.

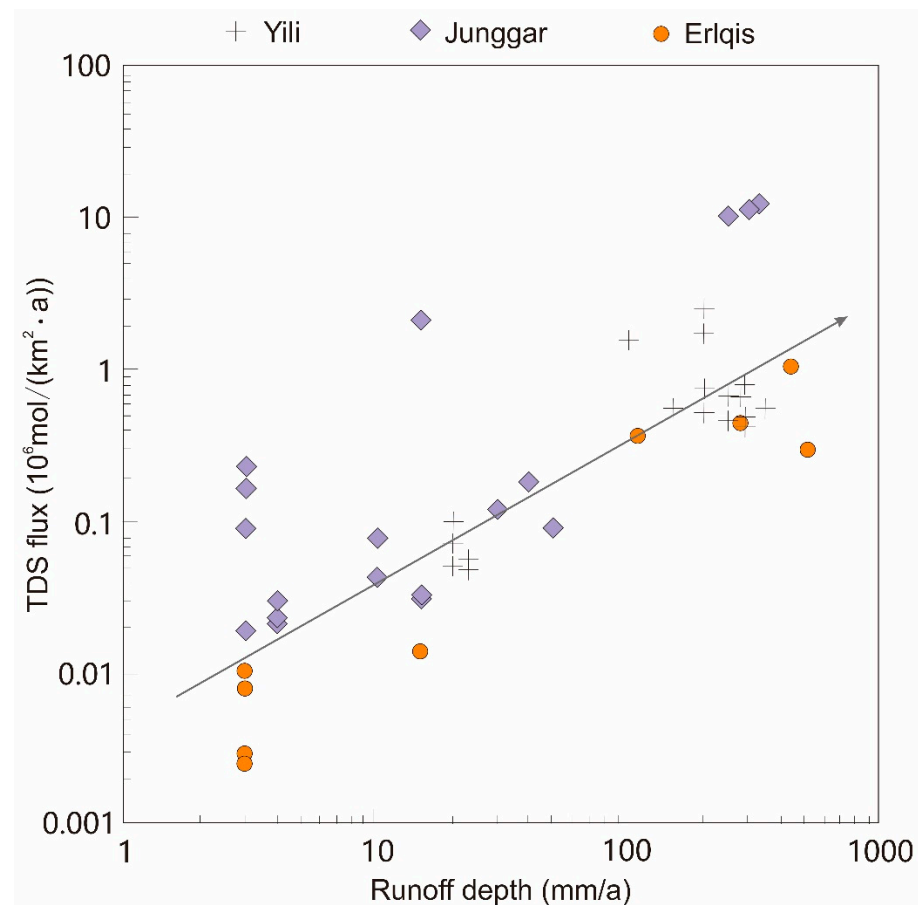


Figure 13. Relationship between the TDS flux and runoff depth of drainage systems in the north of Tianshan Mountains.

It is worth noting that further analysis of ion concentration data shows that as the runoff depth increases, the concentrations of major cations decrease in the three drainage systems in the north of Tianshan Mountains (Figure 14), indicating that the water cations are affected by the dilution effect of runoff. However, the positive correlation between total solute flux and runoff shown in Figure 13 cannot be explained by the dilution effect. This phenomenon indicates that the conditions limiting the chemical weathering rate at a basin scale in the study area are still hydrological factors (runoff and precipitation) and

climatic factors (aridity), because the intensity of water–rock interaction has not reached its maximum and the ion concentration in natural water has not reached its saturation state. This evidence proves that hydroclimatic factors such as runoff and aridity have a strong effect in limiting the process and intensity of chemical weathering in the study area.

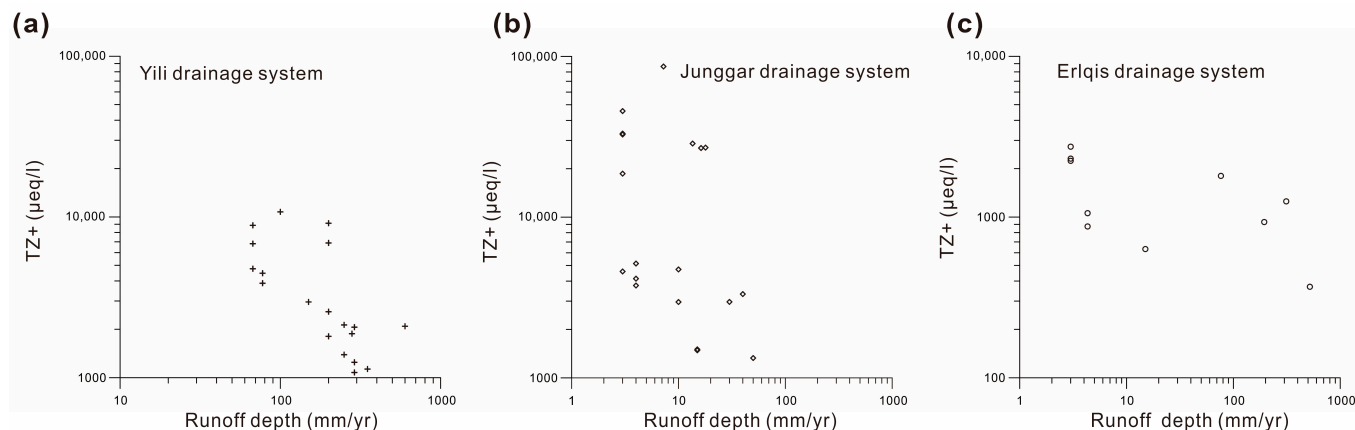


Figure 14. Relationship between runoff depth (mm/yr) and the total cations concentrations (TZ^+) for three drainage systems in the north of the Tianshan Mountains. Parts of data are cited from [36]. (a) TZ^+ vs. runoff depth in the Yili drainage system, (b) TZ^+ vs. runoff depth in the Junggar drainage system, (c) TZ^+ vs. runoff depth in the Erlqis drainage system.

In addition, from the perspective of hydrological divisions of drainage system in the north of the Tianshan Mountains, the following laws are generally observed among the recharge area (mountain snow-covered area), runoff area (foothill and piedmont plain), and discharge area (lowland desert area) of a river basin. The ion concentrations in the recharge area are low, and the solutes are mainly originated from weathering of carbonate rocks and silicate rocks. The solute source in the runoff area is dominated by weathering of carbonate rocks and dissolution of evaporites. The solute source in the discharge area is mainly from the dissolution of evaporites [36]. Generally, the relationship between hydrological zoning and hydrochemical composition should be a comprehensive reflection of multiple influencing factors in essence.

On a global scale, the impact of runoff, as one of the most important hydroclimatic parameters, on chemical weathering is also a highly valued scientific issue. Gailardet et al. [16,98] have suggested that runoff is an important factor second only to lithology in controlling the hydrochemistry at the basin scale. For some basins with certain specific rock types, Suchet and Probst [123] and White [114] hold that the rate of chemical weathering in the basin may be roughly proportional to the runoff. Pinet and Soureau [120] estimated the relationship between chemical weathering rate and runoff in many large basins worldwide, showing a high correlation between the two ($r^2 = 0.59$). After further research, Summerfield and Hulton [102] argued that this correlation coefficient reached 0.52. Based on the hydrochemical study of 60 major rivers in the world, Ludwig and Probst [124] have found that the correlation coefficient between sedimentary load and runoff intensity of these large rivers is as high as 0.7, which is higher than other factors such as temperature, precipitation, and topography. These studies indicate that runoff is generally one of the main factors influencing the water chemistry at the global scale. The positive effect of runoff on driving hydrochemical weathering is usually explained as that the increase of runoff can increase the contact area between water flow and rocks, consequently increasing the intensity and duration of water–rock interaction, thus making the chemical weathering reaction more intense [20,44,107,125].

However, it should be noted that most of the cases mentioned above, whether they are hydrochemical studies of certain catchments with specific rock types or comprehensive

studies of global large rivers, are mostly located in tropical or subtropical regions with relatively rich rainfall, while research records from arid regions are rare.

5.3.3. Lithological Geology

Generally, the processes of water–rock interaction and the flux of hydrochemical solutes vary greatly between basins with different rock types. On a global scale, the estimated result of hydrochemical weathering in small-scale basins with specific rock types is that if the chemical weathering rate of silicate rocks is set as 1, the relative weathering rate of carbonate rocks can be approximately 12, and the average value of evaporate rocks can be 60 [47]. Therefore, the exposed area of global terrestrial carbonate rocks and evaporite rocks accounts for about 17% of the total surface area, but they contribute about 63% of the fluvial solute [125]. In addition, the weathering rate of different rocks of the same lithology is also different, such as in carbonate rocks, and the weathering rate of limestone is significantly higher than that of dolomite [126].

Figures 10 and 11 have revealed that the origin of hydrochemical composition of most areas in the north of the Tianshan Mountains is dominated by rock weathering. According to the lithologic geology map (Figure 1c), although the distribution area of carbonate rocks in the north of the Tianshan Mountains is much smaller than that of silicate rocks, the hydrochemical types of ions in natural water dominated by Ca-HCO₃ and Ca-Mg-HCO₃-SO₄ in this study indicate that the weathering of carbonate rocks contributes more solute content. This is precisely because the carbonate rock has a higher weathering rate than other rocks and the low temperature environment is more conducive to carbonate dissolution [36]. In addition, from the perspective of ion composition and ion distribution characteristics, weathering of carbonate rocks and dissolution of evaporites should be the most important mechanism of rock weathering in the north of Tianshan Mountains. The results of weathering flux calculated for the north of the Tianshan Mountains show that the weathering of silicate rocks has a greater impact on hydrochemistry in the middle and low elevation areas (such as the piedmont plain), while that of carbonate rocks has a greater impact in the high elevation mountainous areas. However, in the areas of the basin with the lowest elevation, such as the Gurbantunggut Desert in the central Junggar Basin, the solute source of natural water (mainly groundwater) is dominated by evaporite dissolution [36].

5.3.4. Physical Erosion

Atmospheric precipitation in the north of the Tianshan Mountains is mainly concentrated in the high elevation mountain areas, while the climate in the lowland plain areas is relatively dry. Under this background, water erosion occurs mostly in the proluvial/diluvial and alluvial fans in the middle- to high-altitude areas. Therefore, physical erosion is considered to mainly occur in the middle- and high-altitude areas, while the lowland plain areas are deposited with thick Quaternary soil/sedimentary layers and the physical erosion is weak [36]. At present, however, few studies have been done to confirm whether this regional erosion feature can indicate that the physical erosion in high altitude areas will promote the hydrochemical process in the north of the Tianshan Mountains, while at the low altitude areas it will restrict the hydrochemical process.

On a geological time scale, although paleo-geographical studies suggest that the impact of active tectonic activities on the erosion process in high altitude regions around the world should be much greater than the effect of climate [102,121], geological records from the north of the Tianshan Mountains have shown that compared to the erosion rates of other mountain ranges in the world, the arid climate in the north of the Tianshan Mountains significantly restricts the erosion of alluvial fans in the Tianshan Mountains [127]. This indicates that although there is a young orogenic system in the Tianshan Mountains, the physical erosion process is not active. Therefore, it is difficult to speculate whether the physical erosion promotes the hydrochemical process in the north of Tianshan Mountains on a long-term scale.

However, some studies have observed a positive correlation between river sediment load (physical erosion) and runoff in the plain area north of the Tianshan Mountains [36], and there is also a clear positive correlation between runoff and hydrochemical solute flux in the north of the Tianshan Mountains in this study (Figure 13), which seems to infer that there is a certain relationship between regional physical erosion and water chemistry. However, judging from the accumulation of existing research work, more detailed study is needed to determine whether physical erosion directly affects the hydrochemical process and its solute flux in the north of Tianshan Mountains.

From a Chinese and global perspective, the relationship between physical erosion and chemical weathering process in different river basins may be uncertain. A comparative study from the Yellow River and the Yangtze River basins [24] has found that strong physical erosion does not promote the chemical weathering process in the Yellow River basin. Studies on paleo-chemical weathering from the Loess Plateau [128,129] even have found a negative correlation between the physical erosion intensity and the chemical weathering rate in the region, indicating that the former has an inhibitory effect on the latter. However, hydrochemical studies from arid environments in northern China, such as river basins at the northwestern and northeastern edges of the Qinghai–Tibet Plateau [130,131], have found no correlation between physical erosion rate and chemical solute flux. Some studies suggest that high-intensity physical erosion may promote the chemical weathering process to a certain extent [16,99,102,118,121], especially in high elevation areas and tectonically active areas. For example, Gaillardet et al. [16] have studied 60 major rivers around the world and found that the intensity of physical erosion has a great impact on hydrochemical process. The weathering rate of silicate rocks in the Yamuna River basin is about twice that of the Ganges River basin, which is thought to be due to the better physical erosion conditions of the Yamuna River [99]. A comparison of chemical weathering between low and high elevation watersheds in Hawaii and Iceland [124] have shown that although there are significant differences in climate between the two watersheds, the solute fluxes are roughly the same. Therefore, it can be inferred that physical erosion may both promote and limit the hydrochemical process. In other words, if the physical erosion rate is higher than the chemical erosion rate, the climate conditions will constrain the hydrochemical process. If the physical erosion rate is lower than the hydrochemical erosion rate, the weathered soil layer will form a protective layer on the rock surface, which will limit the continuation of the hydrochemical erosion process, regardless of whether the climatic conditions are suitable for further weathering. This may contribute to future research on the relationship between physical erosion and chemical weathering in the drainage systems in the north of the Tianshan Mountains and other special river basins.

6. Conclusions

In this paper, three major drainage systems in the north of the Tianshan Mountains were selected for hydrochemical research, in order to understand the hydrochemical composition, ion origins, and their influencing factors of these westerly drainage systems in the CAOBS under an arid environment. The results show that the total dissolved solid concentration (TDS value) of various river systems in the north of Tianshan Mountains is generally higher than that of rivers in China's monsoon and humid regions, and also higher than the world average. The relative concentration of major ions is similar to that of rivers in the monsoon region of eastern China, while the absolute concentration is higher than that of most rivers in the world. Surface water samples of different sub-basins in the study area are distributed near the Ca apex in the piper diagram, while phreatic and confined groundwater samples tend to the Na apex. The magnesium concentrations do not show such a difference among these water types. The compositional variations of the anions are not like the cations, rarely distinguishable for these different water types. In a sub-drainage basin scale (from I to VIII sub-basins in the study area), major ion concentrations and distributions in these basins are evidently heterogeneous. Almost all the cation and anion concentrations span > 1 order of magnitude, especially sodium and chlorine. However, the

calcium and alkalinity concentrations and distributions are relatively homogeneous for some basins in the Junggar and Yili drainage systems. The relative homogeneity between anions and the relative heterogeneity between cations can be recognized in the ion chemistry of natural water samples between different types, indicating that the composition and distribution of cations in water is more conducive than those of anions to identifying the differences and commonalities between different regions. The results of quantitative analysis of contribution sources show that the contribution rate of evaporite dissolution is about 9.8–74.3% (mean 43.6%), that of carbonate rock weathering is about 14.9–44.6% (mean 29.7%), that of silicate rock weathering is about 8.9–26.7% (mean 17.8%), and that of atmospheric precipitation input is about 0.4–45.8% (mean 8.9%). Atmospheric precipitation, evaporation crystallization under arid environment and dissolution of evaporite can play a leading role in local areas. Elevation differentiation of chemical weathering and ion concentrations in the study area is closely related to atmospheric precipitation and its role on the hydrogeochemical process in the north of Tianshan Mountains. The positive correlation between total solute flux and runoff cannot be explained by the dilution effect, indicating that hydroclimatic factors such as runoff and aridity have a strong effect in limiting the process and intensity of chemical weathering in the study area.

Supplementary Materials: The following supporting information can be downloaded at: <https://www.mdpi.com/article/10.3390/atmos14071116/s1>, Table S1: Physical and chemical parameters of water samples collected in northern of the Tianshan Mountains, China (Note: 1 water type: SFW or SW, surface water samples including river water, lake water, reservoirs water, pond water, stream water, snow, ice, rainfall, etc.; PGW or PW, phreatic groundwater samples with aquifer depth < 50 m; CGW or CW, confined groundwater samples with aquifer depth > 50 m or > 100 m. 2 Watershed: EQS, Erlqis watershed; YL, Yili watershed; JG: Junggar watershed; YL-TKS, Tekes Basin in Yili watershed; YL-GNS, Gongnais Basin in Yili; YL-KS, Kashi Basin in Yili; YL-YL, Yili Basin in Yili; JG-THB, Tuha Basin in JG; JG-MNSTB, middle part of the north slope of Tianshan Mountains in JG; JG-ABB, Aibi Lake Basin in JG; JG-EMB, Ermin Basin in JG; WLGB, Wulungu Basin in JG. The specific location and distribution of each sampling site are shown in Figure 3); Table S2: Statistical summary of the physical and chemical parameters determined in each of the subdivided river basins (I to VIII) in north of the Tianshan Mountains, China (Note: The specific location and distribution of each sampling site are shown in Figure 3).

Author Contributions: Conceptualization, B.-Q.Z. and J.-X.Z.; methodology, B.-Q.Z. and J.-X.Z.; software, J.-X.Z.; validation, B.-Q.Z. and J.-X.Z.; formal analysis, B.-Q.Z. and J.-X.Z.; investigation, B.-Q.Z. and J.-X.Z.; resources, B.-Q.Z. and J.-X.Z.; data curation, J.-X.Z.; writing—original draft preparation, B.-Q.Z. and J.-X.Z.; writing—review and editing, B.-Q.Z.; visualization, B.-Q.Z. and J.-X.Z.; supervision, B.-Q.Z.; project administration, B.-Q.Z.; funding acquisition, B.-Q.Z. All authors have read and agreed to the published version of the manuscript.

Funding: This work was financially supported by the Third Xinjiang Scientific Expedition Program (2021XJJK0803), the National Natural Science Foundation of China (No. 41930640), and the Project of the Second Comprehensive Scientific Investigation on the Qinghai–Tibet Plateau (2019QZKK1003).

Data Availability Statement: The authors confirm that the data supporting the findings of this study are available within the article and the related references cited.

Acknowledgments: We thank Xiaoping Yang, Zhangdong Jin, Jinlong Zhou, Qiao Li, and other scholars for their help with the authors' research work.

Conflicts of Interest: The authors declare no conflict of interest.

References

1. Dixon, J.L.; Heimsath, A.M.; Amundson, R. The critical role of climate and saprolite weathering in landscape evolution. *Earth Surf. Process. Landforms* **2009**, *34*, 1507–1521. [[CrossRef](#)]
2. Norton, K.P.; von Blanckenburg, F. Silicate weathering of soil-mantled slopes in an active Alpine landscape. *Geochim. Cosmochim. Acta* **2010**, *74*, 5243–5258. [[CrossRef](#)]
3. Berner, E.K.; Berner, R.A. *Global Environment: Water, Air and Geochemical Cycles*; Prentice-Hall: Prentice-Hall, NJ, USA, 1996; p. 376. [[CrossRef](#)]

4. Ludwig, W.; Probst, J.-L.; Kempe, S. Predicting the oceanic input of organic carbon by continental erosion. *Glob. Biogeochem. Cycles* **1996**, *10*, 23–41. [[CrossRef](#)]
5. Liu, Z.; Dreybrodt, W.; Wang, H. A new direction in effective accounting for the atmospheric CO₂ budget: Considering the combined action of carbonate dissolution, the global water cycle and photosynthetic uptake of DIC by aquatic organisms. *Earth-Sci. Rev.* **2010**, *99*, 162–172. [[CrossRef](#)]
6. Goudie, A.S.; Viles, H.A. Weathering and the global carbon cycle: Geomorphological perspectives. *Earth-Sci. Rev.* **2012**, *113*, 59–71. [[CrossRef](#)]
7. Liu, Z. New progress and prospects in the study of rock-weathering-related carbon sinks. *Chin. Sci. Bull.* **2012**, *57*, 95–102. [[CrossRef](#)]
8. Zeng, S.; Liu, Z.; Kaufmann, G. Sensitivity of the global carbonate weathering carbon-sink flux to climate and land-use changes. *Nat. Commun.* **2019**, *10*, 5749. [[CrossRef](#)]
9. Raymo, M.E.; Ruddiman, W.F.; Froelich, P.N. Influence of late cenozoic mountain-building on ocean geochemical cycles. *Geology* **1988**, *16*, 649–653. [[CrossRef](#)]
10. Raymo, M.E.; Ruddiman, W.F. Tectonic forcing of late Cenozoic climate. *Nature* **1992**, *359*, 117–122. [[CrossRef](#)]
11. Quade, J.; Roe, L.; DeCelles, P.G.; Ojha, T.P. The Late Neogene ⁸⁷Sr/⁸⁶Sr Record of Lowland Himalayan Rivers. *Science* **1997**, *276*, 1828–1831. [[CrossRef](#)]
12. Gislason, S.R.; Oelkers, E.H.; Eiriksdottir, E.S.; Kardjilov, M.I.; Gisladottir, G.; Sigfusson, B.; Snorrason, A.; Elefsen, S.; Hardardottir, J.; Torssander, P.; et al. Direct evidence of the feedback between climate and weathering. *Earth Planet Sci. Lett.* **2009**, *277*, 213–222. [[CrossRef](#)]
13. Kump, L.R.; Brantley, S.L.; Arthur, M.A. Chemical weathering, atmospheric CO₂, and climate. *Annu. Rev. Earth Planet. Sci.* **2000**, *28*, 611–667. [[CrossRef](#)]
14. West, A.J.; Galy, A.; Bickle, M. Tectonic and climatic controls on silicate weathering. *Earth Planet Sci. Lett.* **2005**, *235*, 211–228. [[CrossRef](#)]
15. Molnar, P.; Boos, W.R.; Battisti, D.S. Orographic controls on climate and paleoclimate of Asia: Thermal and mechanical roles for the Tibetan plateau. *Annu. Rev. Earth Planet. Sci.* **2010**, *38*, 77–102. [[CrossRef](#)]
16. Gaillardet, J.; Dupré, B.; Louvat, P.; Allègre, C. Global silicate weathering and CO₂ consumption rates deduced from the chemistry of large rivers. *Chem. Geol.* **1999**, *159*, 3–30. [[CrossRef](#)]
17. Liu, Z.; Dreybrodt, W.; Liu, H. Atmospheric CO₂ sink: Silicate weathering or carbonate weathering? *Appl. Geochem.* **2011**, *26*, S292–S294. [[CrossRef](#)]
18. White, A.F.; Brantley, S.L. The effect of time on the weathering of silicate minerals: Why do weathering rates differ in the laboratory and field? *Chem. Geol.* **2003**, *202*, 479–506. [[CrossRef](#)]
19. Cai, W.-J.; Guo, X.; Chen, C.-T.A.; Dai, M.; Zhang, L.; Zhai, W.; Lohrenz, S.E.; Yin, K.; Harrison, P.J.; Wang, Y. A comparative overview of weathering intensity and HCO₃[−] flux in the world's major rivers with emphasis on the Changjiang, Huanghe, Zhujiang (Pearl) and Mississippi Rivers. *Cont. Shelf Res.* **2008**, *28*, 1538–1549. [[CrossRef](#)]
20. Wu, W.; Zheng, H.; Yang, J.; Luo, C.; Zhou, B. Chemical weathering, atmospheric CO₂ consumption, and the controlling factors in a subtropical metamorphic-hosted watershed. *Chem. Geol.* **2013**, *356*, 141–150. [[CrossRef](#)]
21. Lyu, X.; Tao, Z.; Gao, Q.; Peng, H.; Zhou, M. Chemical weathering and riverine carbonate system driven by human activities in a Subtropical Karst Basin, South China. *Water* **2018**, *10*, 1524. [[CrossRef](#)]
22. Zhang, J.; Huang, W.; Létolle, R.; Jusserand, C. Major element chemistry of the Huanghe (Yellow River), China-weathering processes and chemical fluxes. *J. Hydrol.* **1995**, *168*, 173–203. [[CrossRef](#)]
23. Chen, J.; Wang, F.; Xia, X.; Zhang, L. Major element chemistry of the Changjiang (Yangtze River). *Chem. Geol.* **2002**, *187*, 231–255. [[CrossRef](#)]
24. Yang, S.; Jung, H.-S.; Li, C. Two unique weathering regimes in the Changjiang and Huanghe drainage basins: Geochemical evidence from river sediments. *Sediment. Geol.* **2004**, *164*, 19–34. [[CrossRef](#)]
25. Wu, L.; Huh, Y.; Qin, J.; Du, G.; van Der Lee, S. Chemical weathering in the Upper Huang He (Yellow River) draining the eastern Qinghai-Tibet Plateau. *Geochim. Cosmochim. Acta* **2005**, *69*, 5279–5294. [[CrossRef](#)]
26. Xu, Z.; Liu, C.-Q. Chemical weathering in the upper reaches of Xijiang River draining the Yunnan–Guizhou Plateau, Southwest China. *Chem. Geol.* **2007**, *239*, 83–95. [[CrossRef](#)]
27. Wu, W.; Xu, S.; Yang, J.; Yin, H. Silicate weathering and CO₂ consumption deduced from the seven Chinese rivers originating in the Qinghai-Tibet Plateau. *Chem. Geol.* **2008**, *249*, 307–320. [[CrossRef](#)]
28. Wang, B.; Lee, X.-Q.; Yuan, H.-L.; Zhou, H.; Cheng, H.-G.; Cheng, J.-Z.; Zhou, Z.-H.; Xing, Y.; Fang, B.; Zhang, L.-K.; et al. Distinct patterns of chemical weathering in the drainage basins of the Huanghe and Xijiang River, China: Evidence from chemical and Sr-isotopic compositions. *J. Asian Earth Sci.* **2012**, *59*, 219–230. [[CrossRef](#)]
29. Windley, B.F.; Alexeiev, D.; Xiao, W.; Kröner, A.; Badarch, G. Tectonic models for accretion of the Central Asian Orogenic Belt. *J. Geol. Soc.* **2007**, *164*, 31–47. [[CrossRef](#)]
30. Buckman, S.; Aitchison, J.C. *Tectonic Evolution of Paleozoic Terranes in West Junggar, Xinjiang, NW China*; Geological Society London Special Publications: London, UK, 2004; pp. 101–129. [[CrossRef](#)]
31. Zhou, T.; Yuan, F.; Fan, Y.; Zhang, D.; Cooke, D.; Zhao, G. Granites in the Sawuer region of the west Junggar, Xinjiang Province, China: Geochronological and geochemical characteristics and their geodynamic significance. *Lithos* **2008**, *106*, 191–206. [[CrossRef](#)]

32. Fang, X.; Shi, Z.; Yang, S. Development of Tianshan loess and Gurbantunggut Desert and related aridification of Northern Xinjiang. *Chin. Sci. Bull.* **2002**, *47*, 540–545. [[CrossRef](#)]
33. Zhu, B.; Yu, J.; Qin, X.; Rioual, P.; Liu, Z.; Zhang, Y.; Jiang, F.; Mu, Y.; Li, H.; Ren, X.; et al. The significance of mid-latitude rivers for weathering rates and chemical fluxes: Evidence from northern Xinjiang rivers. *J. Hydrol.* **2013**, *486*, 151–174. [[CrossRef](#)]
34. Zhu, B.; Yang, X.; Rioual, P.; Qin, X.; Liu, Z.; Xiong, H.; Yu, J. Hydrogeochemistry of three watersheds (the Erlqis, Zhungarer and Yili) in northern Xinjiang, NW China. *Appl. Geochem.* **2011**, *26*, 1535–1548. [[CrossRef](#)]
35. Zhu, B.; Yu, J.; Qin, X.; Rioual, P.; Xiong, H. Climatic and geological factors contributing to the natural water chemistry in an arid environment from watersheds in northern Xinjiang, China. *Geomorphology* **2012**, *153–154*, 102–114. [[CrossRef](#)]
36. Zhu, B.; Yu, J.; Qin, X.; Rioual, P.; Zhang, Y.; Liu, Z.; Mu, Y.; Li, H.; Ren, X.; Xiong, H. Identification of rock weathering and environmental control in arid catchments (Northern Xinjiang) of Central Asia. *J. Asian Earth Sci.* **2013**, *66*, 277–294. [[CrossRef](#)]
37. Zhu, B.; Yu, J.; Rioual, P. Geochemical signature of natural water recharge in the Jungar Basin and its response to climate. *Water Environ. Res.* **2016**, *88*, 79–86. [[CrossRef](#)]
38. Zhu, B.; Wang, X.; Rioual, P. Multivariate indications between environment and ground water recharge in a sedimentary drainage basin in northwestern China. *J. Hydrol.* **2017**, *549*, 92–113. [[CrossRef](#)]
39. Liu, Y.-L.; Luo, K.-L.; Lin, X.-X.; Gao, X.; Ni, R.-X.; Wang, S.-B.; Tian, X.-L. Regional distribution of longevity population and chemical characteristics of natural water in Xinjiang, China. *Sci. Total. Environ.* **2014**, *473–474*, 54–62. [[CrossRef](#)]
40. Ma, L. *Geological Atlas of China*; Geological Press: Beijing, China, 2002.
41. Şengör, A.M.C.; Natal'in, B.A.; Burtman, V.S. Evolution of the Altaid tectonic collage and Palaeozoic crustal growth in Eurasia. *Nature* **1993**, *364*, 299–307. [[CrossRef](#)]
42. Xinjiang Bureau of Hydrology and Water Resources. *Overview of Surface Water Resources in Xinjiang*; China Water Conservancy and Hydropower Press: Beijing, China, 2011.
43. Anderson, S.P.; Blum, A.E. Controls on chemical weathering: Small- and large-scale perspectives. *Chem. Geol.* **2003**, *202*, 191–193. [[CrossRef](#)]
44. White, A.F.; Blum, A.E.; Schulz, M.S.; Vivit, D.V.; Stonestrom, D.A.; Larsen, M.; Murphy, S.F.; Eberl, D. Chemical Weathering in a Tropical Watershed, Luquillo Mountains, Puerto Rico: I. Long-Term Versus Short-Term Weathering Fluxes. *Geochim. Cosmochim. Acta* **1998**, *62*, 209–226. [[CrossRef](#)]
45. White, A.F.; Schulz, M.S.; Stonestrom, D.A.; Vivit, D.V.; Fitzpatrick, J.; Bullen, T.D.; Maher, K.; Blum, A.E. Chemical weathering of a marine terrace chronosequence, Santa Cruz, California. Part II: Solute profiles, gradients and the comparisons of contemporary and long-term weathering rates. *Geochim. Cosmochim. Acta* **2009**, *73*, 2769–2803. [[CrossRef](#)]
46. Buss, H.L.; Lara, M.C.; Moore, O.W.; Kurtz, A.C.; Schulz, M.S.; White, A.F. Lithological influences on contemporary and long-term regolith weathering at the Luquillo Critical Zone Observatory. *Geochim. Cosmochim. Acta* **2017**, *196*, 224–251. [[CrossRef](#)]
47. Meybeck, M. Global chemical weathering of surficial rocks estimated from river dissolved loads. *Am. J. Sci.* **1987**, *287*, 401–428. [[CrossRef](#)]
48. Meybeck, M.; Helmer, R. The quality of rivers: From pristine stage to global pollution. *Glob. Planet. Chang.* **1989**, *1*, 283–309. [[CrossRef](#)]
49. Meybeck, M. *Global Occurrence of Major Elements in Rivers: Surface and Ground Water, Weathering, and Soils*; Elsevier-Pergamon: Oxford, UK, 2004; pp. 207–223.
50. White, A.F.; Schulz, M.S.; Lawrence, C.R.; Vivit, D.V.; Stonestrom, D.A. Long-term flow-through column experiments and their relevance to natural granitoid weathering rates. *Geochim. Cosmochim. Acta* **2017**, *202*, 190–214. [[CrossRef](#)]
51. Pawellek, F.; Frauenstein, F.; Veizer, J. Hydrochemistry and isotope geochemistry of the upper Danube River. *Geochim. Cosmochim. Acta* **2002**, *66*, 3839–3853. [[CrossRef](#)]
52. Cai, X.; Qian, Y.; Zhang, Q. A study on the hydrochemical of Barcol Salt Lake in Xinjiang and evaluation of Artemia bar-kolica survival environment. *J. Agri. Coll.* **1994**, *17*, 15–20.
53. Zheng, X.; Liu, J. The composition and origin of salt lake brines in Xinjiang. *Sci. Geogr. Sin.* **1996**, *16*, 115–123. [[CrossRef](#)]
54. Liu, J. Application of by geochemistry model to the determination of mineralization of sandstone type uranium ore. *J. Mineral. Petrol.* **2004**, *24*, 65–70. [[CrossRef](#)]
55. Liu, Z.; Liu, S.; Wang, G. Water-rock interaction simulation of groundwater in the plain of Manasi River Basin, Xinjiang. *Acta Geol. Sin.* **2006**, *80*, 885–892. [[CrossRef](#)]
56. Wu, B. Study on Groundwater System Evolvment Law and Water Environment Effect of Shihezi City. Doctoral Thesis, Xinjiang Agricultural University, Urumqi, China, 2007.
57. Liu, C.; Yang, J.; Chen, X. Quality of irrigation water and soil salinity of the Manas river valley in Xinjiang. *Soils* **2008**, *40*, 288–292. [[CrossRef](#)]
58. Chen, G.; Cai, N.; Liu, J. Study on chemical field characteristics of underground brine in north depression area of Luobupo in Xinjiang Uygur Automous Region. *Shandong Land Resour.* **2013**, *29*, 23–26.
59. Li, Q.; Zhou, J.; Ji, Y. Water-rock interaction simulation of groundwater in north Santang lake of Hami district of Xinjiang. *J. Water Resour. Water Eng.* **2013**, *24*, 29–33.
60. Li, Q. Spatial and Temporal Evolution of Groundwater Quality in the Plain Area of Jungar Basin. Doctoral Thesis, Xingjiang Agricultural University, Urumqi, China, 2014.

61. Li, Q.; Zhou, J.; Gao, Y. Variations of groundwater quality in 2003–2011 in the plain area of north Xinjiang, China. *Earth Sci. Front.* **2014**, *21*, 124–134. [[CrossRef](#)]
62. Li, Q.; Zhou, J.; Gao, Y. Groundwater hydro-geochemistry in Plain of Manasi River Basin, Xinjiang. *Geoscience* **2015**, *29*, 238–244.
63. Wu, J.; Zeng, H.; Ma, L. Analysis on water quality and volume of the baihu lake in the Altay Mountains, Xinjiang. *Arid. Zone Res.* **2013**, *30*, 5–9.
64. Chen, Z.; Du, J.; Zhou, X. Hydrogeochemical changes of mud volcanoes and springs in North Tianshan related to the June 30, 2012 Xinyuan Ms6.6 earthquake. *Earthquake* **2014**, *34*, 97–107. [[CrossRef](#)]
65. Ji, Y.; Jia, R.; Zhou, J. Assessment of groundwater quality and pollution in Ili River Valley of Xinjiang. *Water Sav. Irrig.* **2014**, *12*, 32–36. [[CrossRef](#)]
66. Abdusalam, J.; Wang, X.; Shi, Y. Variation analysis of the chemical characteristics of surface water in Turpan City. *Acta Sci. Circumstantiae* **2015**, *35*, 2481–2486. [[CrossRef](#)]
67. Cheng, F. Evolution of Groundwater Environment and Hydrogeochemical Simulation of Shihezi City. Master's Thesis, Xinjiang Agricultural University, Urumqi, China, 2015.
68. Chen, F. Hydrogeochemical simulation of ground water of Shihezi City. *Northwest Water Power* **2016**, *23*, 18–22. [[CrossRef](#)]
69. Shao, J. Groundwater Circulation and Evolution Pattern in Yili-GongNaiSi Valley of Xinjiang Autonomous Region. Master's Thesis, Chang'an University, Xi'an, China, 2015.
70. Shao, J.; Li, Y.; Wang, W. Indicative effects of hydrochemistry on groundwater circulation in the Yili River Valley of Xin-jiang. *Hydrogeol. Eng. Geol.* **2016**, *43*, 30–35. [[CrossRef](#)]
71. Ye, R. Interaction of Surface Water and Groundwater in Yili-Gongnaisi River Valley. Master's Thesis, Chang'an University, Xi'an, China, 2015.
72. Jiang, W.; Zhao, D.; Wang, G. Hydro-geochemical characteristics and formation of groundwater in Tu-Ha Basin, Xinjiang. *Geoscience* **2016**, *30*, 825–833.
73. Wang, H.; Gu, H.; Jiang, J. Hydrochemical characteristics and origin including isotope technique of the river water in the Yili River Basin, Xinjiang. *Quat. Sci.* **2016**, *36*, 1383–1392. [[CrossRef](#)]
74. Wei, H.; Wu, J.-K.; Shen, Y.-P.; Zhang, W.; Liu, S.-W.; Zhou, J.-X. Hydrochemical characteristics of snow meltwater and river water during snow-melting period in the headwaters of the Ertis River, Xinjiang. *Environ. Sci.* **2016**, *37*, 1345–1352. [[CrossRef](#)]
75. Zeng, Y.; Zhou, J.; Gao, Y. Causes of groundwater pollution and the assessment in Shihezi Area, Xinjiang. *J. Arid. Land Resour. Environ.* **2016**, *30*, 197–202. [[CrossRef](#)]
76. Zhu, S.; Zhang, F.; Zhang, H. The seasonal and spatial variations of water chemistry of rivers in EbinurLake Basin. *Acta Sci. Circumstantiae* **2018**, *38*, 892–899. [[CrossRef](#)]
77. Jiao, S.; Liu, L.; Sun, T. Hydrological characteristics and the atmospheric carbon sink in the chemical weathering processes of the Sanchahe watershed. *Geogr. Res.* **2013**, *32*, 1025–1032.
78. Li, R.; Zhang, F.; Gao, Y. Surface hydrochemistry characteristics and controlling factors in the Ebinur Lake region during dry and wet seasons. *J. Glaciol. Geocryol.* **2016**, *38*, 1394–1403. [[CrossRef](#)]
79. Liu, Y.; Lou, K.; Li, L. Regional differences and geological causes of hydrochemistry of natural water in Xinjiang, China. *Sci. Geogr. Sin.* **2016**, *36*, 794–802. [[CrossRef](#)]
80. He, L. Analysis and countermeasures on the present situation of water resources development and utilization in Yili Riv-er Basin. *Shaanxi Water Resour.* **2019**, *14*, 49–51. [[CrossRef](#)]
81. Zheng, L. The temporal-Spatial Distribution of Snow Properties in North Xinjiang. Master's Thesis, Lanzhou University, Lanzhou, China, 2015.
82. Zhu, B.; Yang, X. The ion chemistry of surface and ground waters in the Taklimakan Desert of Tarim Basin, western China. *Chin. Sci. Bull.* **2007**, *52*, 2123–2129. [[CrossRef](#)]
83. Zhang, J.; Takahashi, K.; Wushiki, H.; Yabuki, S.; Xiong, J.-M.; Masuda, A. Water geochemistry of the rivers around the Taklimakan Desert (NW China): Crustal weathering and evaporation processes in arid land. *Chem. Geol.* **1995**, *119*, 225–237. [[CrossRef](#)]
84. Shao, Y.; Lou, G.; Wang, J. Hydrochemical characteristics and formation causes of main Ions in water of the Keriya River, Xinjiang. *Arid. Zone Res.* **2018**, *35*, 1021–1029. [[CrossRef](#)]
85. Li, W.; Wang, W.; Duan, L. Study of hydro-chemical characteristics and genesis in Kashi Reach of Kizil River Basin in Xin-jiang. *South North Water Transf. Water Sci. Technol.* **2016**, *14*, 159–164. [[CrossRef](#)]
86. Sun, Y.; Zhou, J.; Nai, W. Seasonal variation characteristics and causes of surface water chemistry in Kashgar River Basin, Xinjiang. *J. Arid. Land Resour. Environ.* **2019**, *33*, 130–136. [[CrossRef](#)]
87. Xiao, J.; Jin, Z.; Wang, J. Geochemistry of trace elements and water quality assessment of natural water within the Tarim River Basin in the extreme arid region, NW China. *J. Geochem. Explor.* **2014**, *136*, 118–126. [[CrossRef](#)]
88. Wu, X.; Li, Q.; He, J. Hydrochemical characteristics and inner-year process of upper Heihe River in summer half year. *J. Desert Res.* **2008**, *28*, 1190–1196.
89. Hu, M.; Stallard, R.F.; Edmond, J.M. Major ion chemistry of some large Chinese rivers. *Nature* **1982**, *298*, 550–553. [[CrossRef](#)]
90. Li, J.; Zhang, J. Chemical weathering processes and atmospheric CO₂ consumption in the yellow river drainage basin. *Mar. Geol. Quat. Geol.* **2003**, *23*, 43–49. [[CrossRef](#)]
91. Zhao, L.; Yongji, Z.; Zhang, L. Consumption of atmospheric CO₂ via chemical weathering and DIC flux in the Qing-hai-Tibet Plateau major tributaries of the Yellow River. *Period. Ocean. Univ. China* **2017**, *47*, 16–26. [[CrossRef](#)]

92. Li, J.; Zhang, J. Variations of solid content and water chemistry at Nantong Station and weathering processes of the Changjiang Watershed. *Resour. Environ. Yangtze Basin* **2003**, *12*, 363–369. [[CrossRef](#)]
93. Sun, M. Silicate Weathering Rate and Its Controlling Factors: The Study from the Different “Small Watershed Systems”. Master’s Thesis, Nanjing University, Nanjing, China, 2018.
94. Gordeev, V.V.; Martin, J.M.; Sidorov, I.S.; Sidorova, M.V. A reassessment of the Eurasian river input of water, sediment, major elements, and nutrients to the Arctic Ocean. *Am. J. Sci.* **1996**, *296*, 664–691. [[CrossRef](#)]
95. Mast, M.A.; Drever, J.I.; Baron, J. Chemical Weathering in the Loch Vale Watershed, Rocky Mountain National Park, Colorado. *Water Resour. Res.* **1990**, *26*, 2971–2978. [[CrossRef](#)]
96. Kempe, S. Long-term records of CO₂ pressure fluctuations in fresh waters. In *Transport of Carbon and Minerals in Major World Rivers*; Degens, E.T., Ed.; Scope/Unep Sonderband Heft: Hamburg, Germany, 1982; pp. 91–332.
97. Stallard, R.F.; Edmond, J.M. Geochemistry of the Amazon: 3. Weathering chemistry and limits to dissolved inputs. *J. Geophys. Res. Atmos.* **1987**, *92*, 8293–8302. [[CrossRef](#)]
98. Gaillardet, J.; Dupre, B.; Allegre, C.J.; Négrel, P. Chemical and physical denudation in the Amazon River Basin. *Chem. Geol.* **1997**, *142*, 141–173. [[CrossRef](#)]
99. Dalai, T.; Krishnaswami, S.; Sarin, M. Major ion chemistry in the headwaters of the Yamuna river system: Chemical weathering, its temperature dependence and CO₂ consumption in the Himalaya. *Geochim. Cosmochim. Acta* **2002**, *66*, 3397–3416. [[CrossRef](#)]
100. Bastia, F.; Equeenuddin, S. Chemical weathering and associated CO₂ consumption in the Mahanadi river basin, India. *J. Asian Earth Sci.* **2018**, *174*, 218–231. [[CrossRef](#)]
101. Glińska-Lewczuk, K.; Cymes, I. The use of water quality indices (WQI and SAR) for multipurpose assessment of water in dam reservoirs. *J. Elementology* **2012**, *21*, 1211–1224. [[CrossRef](#)]
102. Summerfield, M.A.; Hulton, N.J. Natural controls of fluvial denudation in major world drainage basins. *J. Geophysical Res.* **1994**, *99*, 13871–13883. [[CrossRef](#)]
103. Han, G.; Liu, C.-Q. Water geochemistry controlled by carbonate dissolution: A study of the river waters draining karst-dominated terrain, Guizhou Province, China. *Chem. Geol.* **2004**, *204*, 1–21. [[CrossRef](#)]
104. Wu, W. Hydrochemistry of inland rivers in the north Tibetan Plateau: Constraints and weathering rate estimation. *Sci. Total Environ.* **2016**, *541*, 468–482. [[CrossRef](#)] [[PubMed](#)]
105. Yang, X.; Williams, M.A. The ion chemistry of lakes and late Holocene desiccation in the Badain Jaran Desert, Inner Mongolia, China. *Catena* **2003**, *51*, 45–60. [[CrossRef](#)]
106. Gibbs, R.J. Mechanisms controlling world water chemistry. *Science* **1970**, *170*, 1088–1090. [[CrossRef](#)]
107. White, A.F.; Blum, A.E. Effects of climate on chemical weathering in watersheds. *Geochim. Cosmochim. Acta* **1995**, *59*, 1729–1747. [[CrossRef](#)]
108. Zhang, L.; Gao, M. Research on the distribution characteristics of the population in Xinjiang based on GIS. *Chin. Agric. Sci. Bull.* **2014**, *30*, 301–307.
109. Feth, J.H.; Gibbs, R.J. Mechanisms controlling world water chemistry: Evaporation-crystallization process. *Science* **1971**, *172*, 870–871. [[CrossRef](#)] [[PubMed](#)]
110. Beck, K.; Reuter, J.; Perdue, E. Organic and inorganic geochemistry of some coastal plain rivers of the southeastern United States. *Geochim. Cosmochim. Acta* **1974**, *38*, 341–364. [[CrossRef](#)]
111. Millero, F.J. The physical chemistry of seawater. *Annu. Rev. Earth Planet. Sci.* **1974**, *2*, 101–150. [[CrossRef](#)]
112. Wu, Y.; Gibson, C. Mechanisms controlling the water chemistry of small lakes in Northern Ireland. *Water Res.* **1996**, *30*, 178–182. [[CrossRef](#)]
113. Tang, J.; Xue, H.; Yu, X. The preliminary study on chemical characteristics of precipitation at Mt. Waliguan. *Acta Sci. Circumstantian* **2000**, *20*, 420–425. [[CrossRef](#)]
114. White, A.F. Effects of climate on chemical weathering in watersheds underlain by granitoid rocks. *Miner. Mag.* **1994**, *58A*, 967–968. [[CrossRef](#)]
115. Huh, Y.; Tsoi, M.-Y.; Zaitsev, A.; Edmond, J.M. The fluvial geochemistry of the rivers of Eastern Siberia: I. tributaries of the Lena River draining the sedimentary platform of the Siberian Craton. *Geochim. Cosmochim. Acta* **1998**, *62*, 1657–1676. [[CrossRef](#)]
116. Huh, Y.; Panteleyev, G.; Babich, D.; Zaitsev, A.; Edmond, J.M. The fluvial geochemistry of the rivers of Eastern Siberia: II. Tributaries of the Lena, Omoloy, Yana, Indigirka, Kolyma, and Anadyr draining the collisional/accretionary zone of the Verkhoyansk and Cherskiy ranges. *Geochim. Cosmochim. Acta* **1998**, *62*, 2053–2075. [[CrossRef](#)]
117. Huh, Y.; Edmond, J.M. The fluvial geochemistry of the rivers of Eastern Siberia: III. Tributaries of the Lena and Anabar draining the basement terrain of the Siberian Craton and the Trans-Baikal Highlands. *Geochim. Cosmochim. Acta* **1999**, *63*, 967–987. [[CrossRef](#)]
118. Riebe, C.S.; Kirchner, J.W.; Finkel, R.C. Erosional and climatic effects on long-term chemical weathering rates in granitic landscapes spanning diverse climate regimes. *Earth Planet. Sci. Lett.* **2004**, *224*, 547–562. [[CrossRef](#)]
119. Dinis, P.A.; Garzanti, E.; Hahn, A.; Vermeesch, P.; Cabral-Pinto, M. Weathering indices as climate proxies. A step forward based on Congo and SW African river muds. *Earth-Sci. Rev.* **2019**, *201*, 103039. [[CrossRef](#)]
120. Pinet, P.; Souriau, M. Continental erosion and large-scale relief. *Tectonics* **1988**, *7*, 563–582. [[CrossRef](#)]
121. Edmond, J.M.; Huh, Y. *Chemical Weathering Yields from Basement and Orogenic Terrains in Hot and Cold Climates*. Ruddiman W F. *Tectonic Uplift and Climate Change*; Springer: Boston, MA, USA, 1997; pp. 329–351. [[CrossRef](#)]

122. Riebe, C.S.; Kirchner, J.W.; Granger, D.E. Strong tectonic and weak climatic control of long-term chemical weathering rates. *Geology* **2001**, *29*, 511–514. [[CrossRef](#)]
123. Suchet, P.A.; Probst, J. Modelling of atmospheric CO₂ consumption by chemical weathering of rocks: Application to the Garonne, Congo and Amazon basins. *Chem. Geol.* **1993**, *107*, 205–210. [[CrossRef](#)]
124. Ludwig, W.; Probst, J.-L. River sediment discharge to the oceans; present-day controls and global budgets. *Am. J. Sci.* **1998**, *298*, 265–295. [[CrossRef](#)]
125. Bluth, G.J.; Kump, L.R. Lithologic and climatologic controls of river chemistry. *Geochim. Cosmochim. Acta* **1994**, *58*, 2341–2359. [[CrossRef](#)]
126. Blum, J.D. *The Effect of Late Cenozoic Glaciation and Tectonic Uplift on Silicate Weathering Rates and the Marine 87Sr/86Sr Record*. Ruddiman W F. *Tectonic Uplift and Climate Change*; Springer: Boston, MA, USA, 1997; pp. 259–288. [[CrossRef](#)]
127. Liu, Z.; Dreybrodt, W.; Li, H. Comparison of dissolution rate-determining mechanisms between limestone and dolomite. *J. China Univ. Geosci. Earth Sci.* **2006**, *31*, 131–136. [[CrossRef](#)]
128. Guerit, L.; Barrier, L.; Jolivet, M.; Fu, B.; Métivier, F. Denudation intensity and control in the Chinese Tian Shan: New constraints from mass balance on catchment-alluvial fan systems. *Earth Surf. Process. Landforms* **2015**, *41*, 1088–1106. [[CrossRef](#)]
129. Yang, J.; Chen, J.; An, Z.; Shields, G.; Tao, X.; Zhu, H.; Ji, J.; Chen, Y. Variations in 87Sr/86Sr ratios of calcites in Chinese loess: A proxy for chemical weathering associated with the East Asian summer monsoon. *Palaeogeogr. Palaeoclim. Palaeoecol.* **2000**, *157*, 151–159. [[CrossRef](#)]
130. Yang, J.; Chen, J.; Li, C. Variations in continental weathering intensity over the past 2.5 Ma. *Geol. Rev.* **2000**, *46*, 472–480. [[CrossRef](#)]
131. Ren, X.Z. *Graphic Expression, MATLAB Implementation and Its Application for Hydrochemistry in Natural Water Bodies*; Xi'an Jiaotong University Press: Xi'an, China, 2021.

Disclaimer/Publisher's Note: The statements, opinions and data contained in all publications are solely those of the individual author(s) and contributor(s) and not of MDPI and/or the editor(s). MDPI and/or the editor(s) disclaim responsibility for any injury to people or property resulting from any ideas, methods, instructions or products referred to in the content.